ORIGINAL PAPER

Effectiveness of Ti-in-amphibole thermometry and performance of different thermometers across lower continental crust up to UHT metamorphism

Omar Bartoli[1] · Bruna B. Carvalho[1] · Federico Farina[2]

Abstract

Metabasites are important constituents of deep crustal sections and are the favored rock type for studying lower crustal amphibolite to granulite transitions. However, metapelites may develop a larger number of temperature-sensitive mineral assemblages and are particular useful when extreme ultrahigh temperature (UHT) conditions are envisaged. A recent calibration of the Ti-in-amphibole thermometer by Liao et al. (2021) was supposed to make thermometry on metabasites quick and easy to apply. However, their calibration is based on experiments which were not originally designed to investigate in detail the temperature dependence of Ti in amphibole. In addition, a possible effect of a_{TiO2} and/or pressure on the Ti content of amphibole was not fully taken into account. This resulted in a calibration uncertainty of ± 70 °C (2σ), much higher than that of other single-mineral thermometers. In this study we firstly test the newly calibrated Ti-in-amphibole thermometer across the mid to lower crustal section of the Ivrea–Verbano Zone (IVZ; NW Italy) and compare the performance of different thermometric techniques across the sequence. Ti-in-amphibole thermometry records increasing peak temperatures from amphibolite (600–700 °C), transition (750–800 °C) and granulite (850–950 °C) zones. Titanium content of amphibole may be modified by retrograde fluid influx returning temperatures c. 200–300 °C lower than in non-altered domains. The comparison reveals that Zr-in-rutile thermometer in pelitic granulites seems to be more prone to post-peak resetting than the Ti-in-amphibole thermometry in nearby mafic rocks. This behavior is also confirmed by amphibole analyses from other UHT localities, where the performance of Ti-in-amphibole thermometry is comparable with that of Al-in-orthopyroxene in pelitic granulites. However, Ti-in-amphibole temperatures are underestimated in rutile-bearing samples and this limitation is not solely restricted to rocks containing high H_2O contents as previously thought. Derived constraints on the diffusivity of Ti through amphibole demonstrate the robustness of the Ti-in-amphibole thermometer to later thermal disturbances. However, ad-hoc experiments are still necessary to improve the accuracy and precision of calibration and to extend its applicability. This advance will make mafic granulites routine targets for studies devoted to understanding the regional extent of UHT metamorphism.

Keywords Ti-in-amphibole · Metabasite · Thermometry · Ivrea–Verbano Zone · Granulite · UHT metamorphism

Introduction

One of the main goals of metamorphic petrology is to unravel the pressure and temperature evolution of metamorphic terranes, often adding these important pieces of information to temporal and microstructural constraints to recover complete P–T–D–t paths. In the high- to ultrahigh temperature realm, getting robust constraints on maximum temperatures is crucial to gain a better understanding on the heat source and tectonic settings where extremely high crustal temperatures (> 900–950 °C) are achieved, a topic

stirring a considerable debate (Clark et al. 2011; Harley 2021; Jiao et al. 2023). Moreover, knowing the thermal evolution of metamorphic terranes is crucial for interpreting the significance of geochronological data (Yakymchuk and Brown 2014). Limitations of conventional element exchange thermometry for granulites (Frost and Chacko 1989; Spear 1991) were circumvented (1) correcting for the effects of late Fe–Mg exchange (Pattison et al. 2003, 2019), (2) calculating P–T pseudosections with the most up-to-date activity-composition (a–x) models for key minerals in residual granulites (Wheller and Powell 2014), (3) applying single-mineral thermometers, such as Zr-in-rutile, Al-in-orthopyroxene and ternary feldspar thermometry, among the others (e.g., Harley and Green 1982; Tomkins et al. 2007), or (4) by applying a hybrid approach of phase equilibria modelling and quadrivalent (4+) cation trace element thermometry (e.g., Korhonen et al. 2015; Dharmapriya et al. 2021).

Metabasic rocks are considered a key rock type to investigate lower crustal metamorphism (e.g., Bohlen and Essene 1979; Clough and Field 1980; Raase et al. 1986; Raith and Raase 1986; Waters 1988; Sawyer 1991). Recent improvements of a–x models for complex solutions such as amphibole and clinopyroxene, along with the development of a model for melt of broadly trondhjemitic–tonalitic composition (Green et al. 2016), has allowed high temperature (HT) to ultrahigh temperature (UHT) equilibria in metabasic systems to be properly calculated (Palin et al. 2016; Kunz and White 2019). Despite this important step forward for interpreting the petrological evolution of mafic migmatites and granulites, consistent discrepancies have been reported in the literature between observed compositions and modal abundances of amphibole and clinopyroxene and those calculated applying the most recent a–x models (Forshaw et al. 2019; Santos et al. 2019). Indeed, a–x formulations of these complex phases suffer from the large uncertainties of thermodynamic mixing properties, which inevitably affect the reliability and accuracy of phase equilibria calculations (Lanari and Duesterhoeft 2019). This, in turn, may lead to a knock-on effect on the predicted stability of other phases (Forshaw et al. 2019; Schorn and Diener 2019). For these reasons, single-mineral thermometers, whose associated uncertainties are generally quantified (e.g., Tomkins et al. 2007; Kohn 2020), are fundamental tools for metamorphic petrologists, being often preferred to phase equilibria modeling (Qi et al. 2022).

Regarding metabasic systems, Liao et al. (2021) recently calibrated a new Ti-in-amphibole thermometer to recover crystallization temperature in igneous and high-grade metamorphic rocks in the presence of Ti-phases (ilmenite, rutile, or titanite). Its alleged independence from pressure and the low diffusivity of Ti in silicates (up to 1–3 orders

of magnitude slower than those of Mg and Fe; Cherniak and Liang 2012) are considered to be the main strengths of Ti-in-amphibole thermometer. Moreover, amphibole may survive up to 950–1000 °C during prograde metamorphism and melting of basic rocks (Fig. 1a), independently from the prograde P–T path and the closed- vs. open-system behavior of the rock (Rushmer 1991; Wolf and Wyllie 1993; Rapp and Watson 1995; Kunz and White 2019; Huang et al. 2021). These characteristics make this thermometer a potentially powerful tool in recovering thermal history of mafic migmatitic and granulitic terranes (e.g., Aidoo et al. 2022; Corvò et al. 2022; Duan et al. 2023; Li et al. 2022).

Here, we delve deeply into the calibration of Ti-in-amphibole thermometer proposed by Liao et al. (2021) and apply this thermometric technique to the mid amphibolite- to granulite-facies mafic rocks of the archetypal continental crustal section of the Ivrea–Verbano Zone (IVZ; NW Italy). Peak temperatures attained across this sequence are well constrained by a combination of different thermometric techniques (P–T pseudosections, classical and quadrivalent (4+) cation trace element thermometry) applied to these rocks over the last > 50 years (e.g., Reinsch 1973; Hunziker and Zingg 1980; Sills 1984; Henk et al. 1997; Luvizotto and Zack 2009; Redler et al. 2012; Ewing et al. 2013; Kunz and White 2019). After interpreting the variability of Ti-in-amphibole temperatures among samples and within the same thin section, the performance of different thermometers across the IVZ crustal section is compared. We then combine amphibole data collected in this study with those from other renowned UHT localities to obtain a more comprehensive overview of the effectiveness of Ti-in-amphibole thermometry up to extreme crustal conditions. Lastly, on the basis of what is known about the cooling history of the IVZ, we speculate on the diffusivity of Ti in amphibole.

Ti-in-amphibole thermometry: a critical assessment

Taking advantage of previous studies which show a relationship between temperature and the Ti content of amphibole (e.g., Leake 1965; Raase 1974; Otten 1984; Ernst and Liu 1998), Liao et al. (2021) proposed a new calibration for the thermometer based on Ti content of calcium amphibole. These authors used both crystallization and melting experiments from the literature, with pressure and temperature in the range 2–20 kbar and 700–1000 °C, respectively (Fig. 1a). Following their recommendations, this thermometer should be applied to subalkaline systems when amphibole is in equilibrium with Ti-phases (ilmenite, rutile or titanite) at ΔNNO $\leq$ 2. Liao et al. (2021) state that Ti-in-amphibole thermometry is likely (i) to overestimate temperature when applied to subsolidus H_2O-undersaturated rocks with low (< 1.5 wt%) H_2O content, or (ii) to underestimate
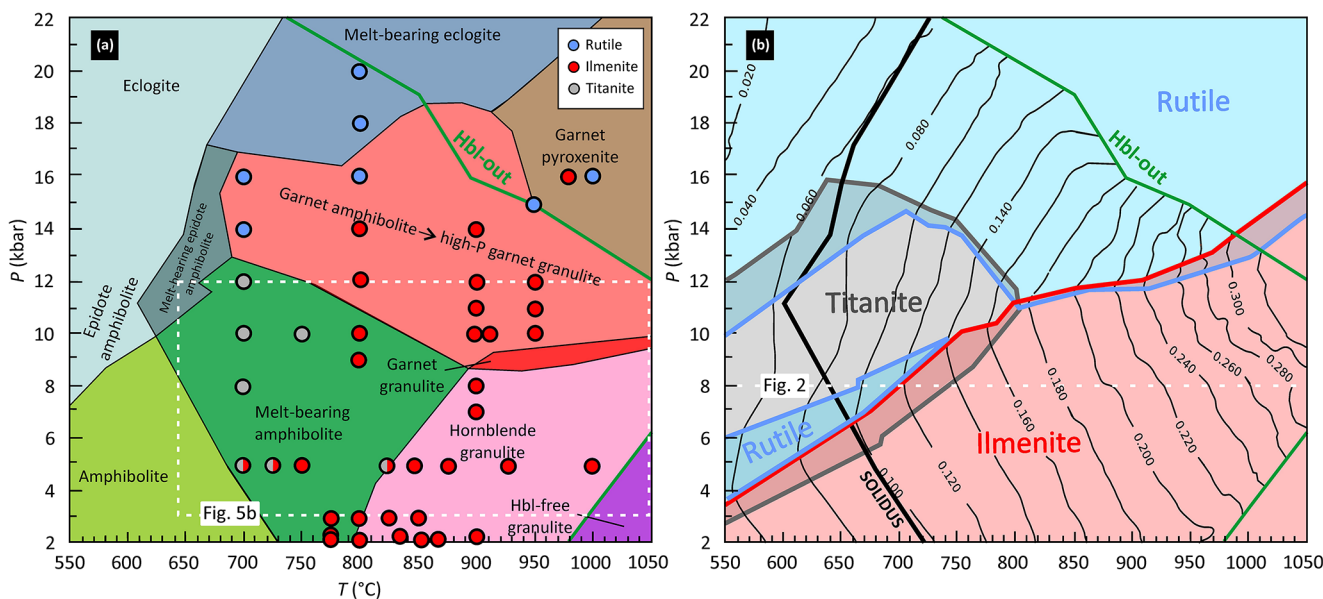
Fig. 1 (**a**) Petrological diagram constructed from a P–T pseudosection calculated for a tholeiitic bulk composition. (redrawn from Palin et al. 2016). Green line marks the limit of amphibole stability. Colored dots reflect the P–T conditions of experimental datasets used by Liao et al. (2021) to calibrate the Ti-in-amphibole thermometer; color coding identifies the Ti-phase present in the experimental run. Dashed white line reflects the P–T window of Fig. 5b. (**b**) Predicted isopleths (black thin lines) for Ti content of amphibole for the tholeiitic bulk composition reported in (**a**). Calculations were performed using Perple_X software (Connolly 2009) using solution models reported in Palin et al. (2016). The stability fields of rutile, ilmenite and titanite are also shown by light blue, red and grey areas and lines. Green line as in (**a**). The dashed white line at 8 kbar marks the P and T conditions at which the diagram of Fig. 2 was calculated

temperature for rocks equilibrated at > 850 °C, in the rutile stability field and containing high (> 3.5 wt%) H_2O content. The standard error (1σ) of calibration was quantified to be ± 35 °C.

Despite the few potential limitations reported above, the general applicability of Ti-in-amphibole thermometry to high-grade metamorphic terrains remains uncertain. Only 15% of experiments used for the calibration were run at > 900 °C (Fig. 1a) and the R^2 value of 0.84 obtained from the nonlinear fitting of the experimental dataset is worse than R^2 reported for other single-mineral thermometers. For instance, the regression for the Zr-in-rutile calibration has a R^2 value of 0.99 (see Kohn 2020). This discrepancy is also evident considering the calibration error: Liao et al. (2021) reported a 1σ value of ± 35 °C, i.e., ± 70 °C (2σ), much higher than 20–30 and 10–15 °C (2σ) documented by Kohn (2020) for different calibrations of the Zr-in-rutile thermometer.

Regarding Ti-in-amphibole thermometry, one important unresolved issue is whether a_{TiO2} and pressure may affect the Ti content of amphibole or not. Models predict a marked change of the slope of isopleths for Ti content in amphibole from ilmenite- to titanite and rutile-bearing mineral assemblages (Fig. 1b). The possible a_{TiO2} dependence of Ti-in-amphibole thermometry would open the door to another potential source of uncertainty. Indeed, the activity of titania has to be considered a dynamic parameter in rutile-absent
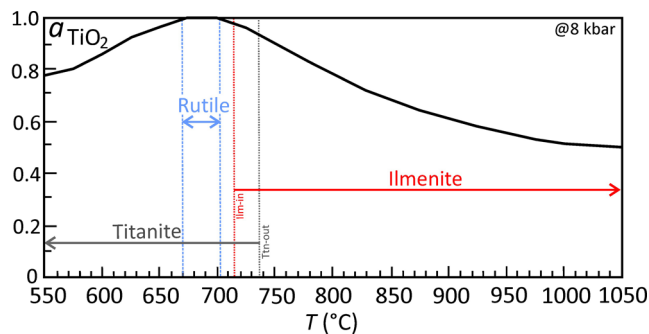

Fig. 2 T-a_{TiO2} diagram calculated at 8 kbar (see Fig. 1b). The stability fields for rutile, titanite and ilmenite are shown

systems, even though other Ti-phases (ilmenite and/or titanite) are present (Fig. 2). Different reaction sequences impact on the amount of ilmenite/titanite whose modal variations impose different values for bulk rock a_{TiO2} (Fig. 2). Also the TiO_2 of melt may impact on a_{TiO2} (Fonseca Texeira et al. 2023). However, this aspect cannot be explored with the melt model proposed by Green et al. (2016) for metabasites, because it does not consider TiO_2. The melt model released later by Holland et al. (2018) has a TiO_2 end member, but it seems to overestimate the TiO_2 content of melt when compared to experimental runs (García-Arias 2020).

The experimental dataset constructed by Liao et al. (2021) implicitly assumes that pressure does not play a role in controlling the Ti content of amphibole (Fig. 3a, b), even
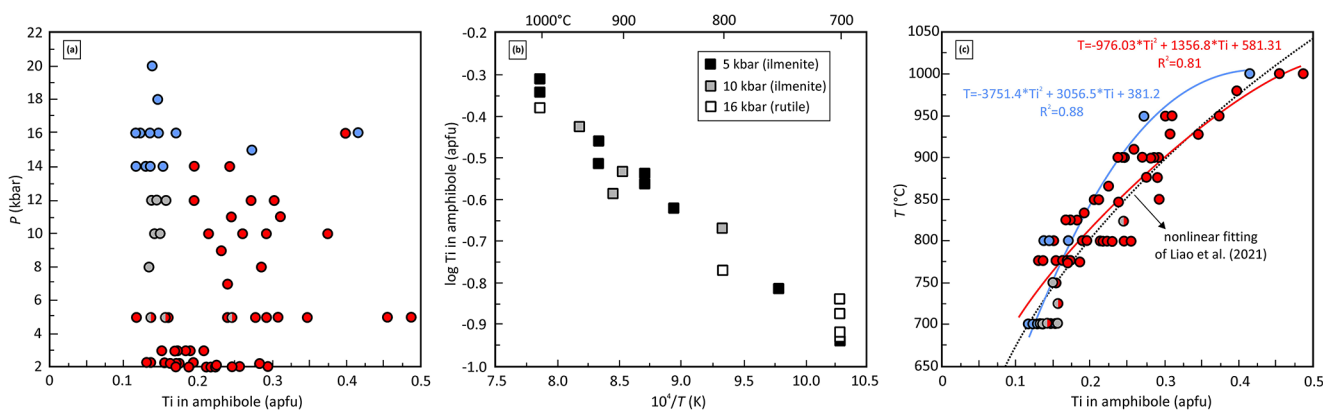
Fig. 3 Diagrams showing *T, P* and Ti content of amphibole from the experimental dataset used by Liao et al. (2021) to calibrate the Ti-in-amphibole thermometer. Colored symbols in (**a**) and (**c**) refer to the different Ti-phases present in experimental runs (symbols as in Fig. 1a). (**b**) Arrhenius plot of Ti-in-amphibole contents considering experimental runs at 5, 10 and 16 kbar, where ilmenite, titanite or rutile were present. In (**c**), regression curves and related equations are shown for both ilmenite- and rutile- bearing datasets. The nonlinearl fitting of Liao et al. (2021) is reported for comparison

though no experimental studies have been conducted to specifically explore this aspect. Only 18% of experimental runs (i.e., 13 over 72 among those considered by Liao et al. 2021) generated a product in which amphibole is present together with rutile (Figs. 1 and 3a) and Liao et al. (2021) did not consider separately the two datasets (rutile-bearing vs. -absent) when they calibrated this thermometer. However, two different second-order polynomial least squares regression curves can be fitted for the two datasets, suggesting that the equation proposed by Liao et al. (2021) could underestimate temperature when amphibole is in equilibrium with rutile (Fig. 3c), whatever the bulk H_2O content is. For instance, the two empirical equations reported in Fig. 3c for rutile- and ilmenite-bearing systems provide temperature estimates of 960 and 900 °C, respectively, for the same Ti content in amphibole of 0.30 apfu. Instead, Liao's equation yields 902 °C, in agreement with their calibration being more appropriate for ilmenite-bearing metabasites.

Further issues that should be tackled are: models presented by Liao et al. (2021) exclude a dependence of Ti content of amphibole from bulk rock composition; however, this aspect has not been evaluated in natural samples. In addition, is Ti content of amphibole susceptible to post-peak resetting? If yes, to what extent and through what processes? For instance, other single-mineral thermometers based on the temperature-dependent incorporation of Ti have been demonstrated to be potentially susceptible to diffusive modification of Ti when applied to slowly cooled rocks with peak temperature > 800 °C – e.g., Ti-in-garnet (Ague and Eckert 2012) and Ti-in-zircon (Bloch et al. 2022). Therefore, it is essential to assess the utility and effectiveness of the Ti-in-amphibole thermometer in high-grade metamorphic terranes up to UHT conditions.

Geological background and sampling

The IVZ (NW Italy) is a well-preserved section of the Carboniferous-Permian continental crust (e.g. Zingg et al. 1990; Quick et al. 1995) that was attenuated during the Mesozoic rifting of the Adriatic microcontinent (e.g. Henk et al. 1997; Handy et al. 1999; Smye and Stockli 2014; Ewing et al. 2015) and tilted during the Alpine collision (Handy et al. 1999; Rutter et al. 2007; Siegesmund et al. 2008; Wolff et al. 2012). The IVZ belongs to the South Alpine domain and it is juxtaposed against the Sesia Zone by the Cenozoic Insubric Line to the NW (Fig. 5). Towards the SE, the IVZ is separated from the upper crust of the Strona-Ceneri Zone by the late-Variscan Cossato-Mergozzo-Brissago Line (CMB) and, in places, the Triassic-Jurassic Pogallo Line (PL) (Schmid et al. 1987; Boriani et al. 1990; Zingg et al. 1990).

The IVZ is composed of ultramafic rocks (Balmuccia and Finero peridotites), the Mafic Complex and the Kinzigite Formation (Fig. 4; see Schmid and Wood 1976; Zingg 1983; Schmid 1993; Quick et al. 2003). The Mafic Complex consists of gabbros, diorites and norites (Rivalenti et al. 1975; Voshage et al. 1990; Mazzuchelli et al. 1992; Sinigoi et al. 1991, 1994) which underplated the lower crustal rocks of the Kinzigite Formation during the Permian (c. 282–286 Ma), coevally with the granitic magmatism and acid volcanism in the upper crust (Peressini et al. 2007; Karakas et al. 2019). Within the Mafic Complex, Sinigoi et al. (1996) identified the "paragneiss-bearing belt", consisting of metapelitic slivers (septa) derived from the Kinzigite Formation and incorporated into the Mafic Complex.

The Kinzigite Formation consists of interlayered metapelites and metabasites with subordinate metapsammites, calcsilicates and marbles (Bertolani 1968; Schmidt 1993) and is best exposed in Val Strona di Omegna (Fig. 4).
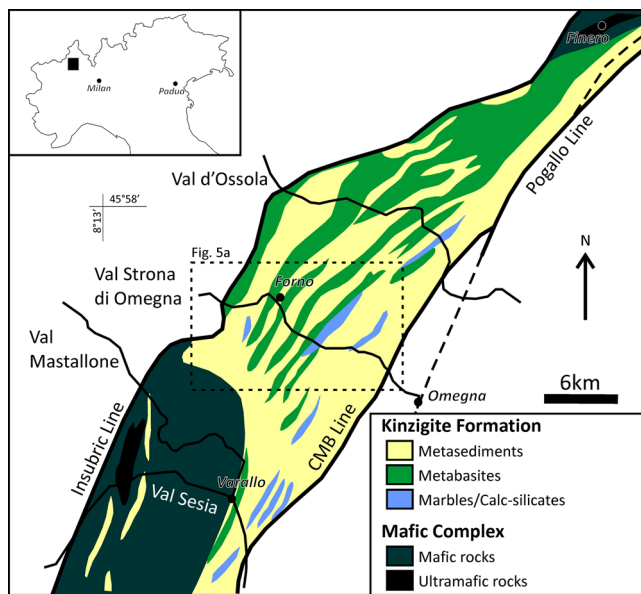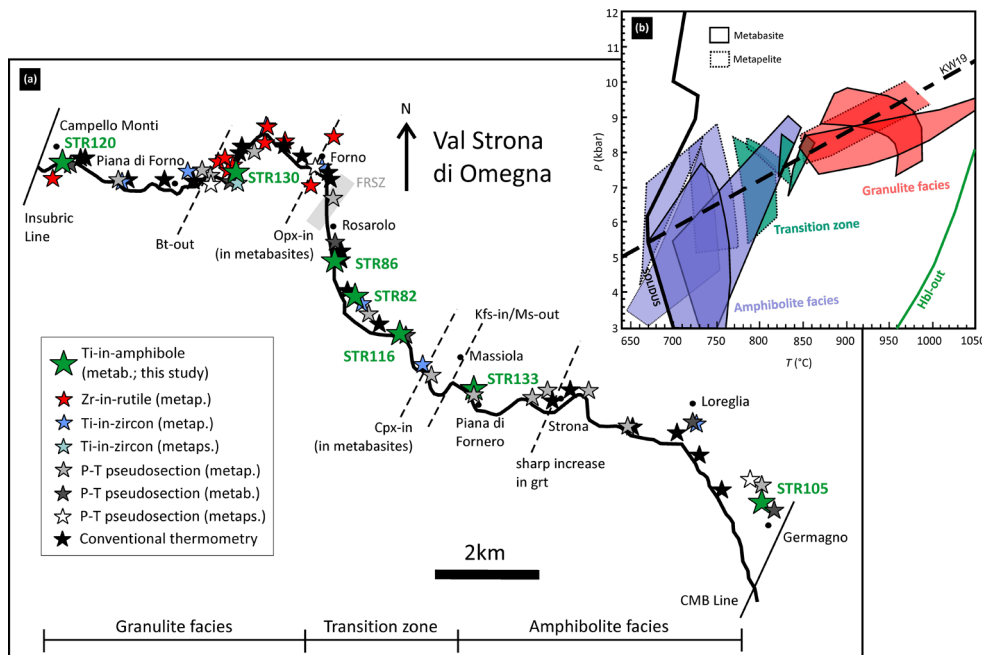
Fig. 4 Geological overview map of the Ivrea-Verbano Zone (redrawn after Kunz and White 2019)

Here, the Kinzigite Formation has been subdivided from SE to NW into three sections on the basis of the metamorphic grade (Fig. 5a): an amphibolite facies zone, a transition zone and a granulite facies zone (Bea and Montero 1999; Redler et al. 2012). The upper and lower boundary of the transition zone is marked by Opx-in and Ms-out isograds in metabasite and metapelite, respectively (mineral abbreviations after Whitney and Evans 2010). The appearance of clinopyroxene in metabasic rocks (Cpx-in) occurs close to the Ms-out isograd in metapelites (Fig. 5a). The sequence displays a continuous metamorphic field gradient (Fig. 5b)

perpendicular to the dominant planar fabric, with metamorphic conditions ranging from mid-amphibolite facies ($\approx 650\,°C$, ≈ 5 kbar) in the SE to granulite facies ($> 900\,°C$, ≈ 10 kbar) in the NW, adjacent to the Insubric Line (e.g., Schmid and Wood 1976; Sills 1984; Henk et al. 1997; Luvizotto and Zack 2009; Redler et al. 2012, 2013; Ewing et al. 2013; Kunz and White 2019). The highest temperatures ($> 1000\,°C$) for IVZ crustal rocks have been recorded by rutile of metapelitic septa (Ewing et al. 2013; Pape et al. 2016).

Regional amphibolite to granulite facies metamorphism likely started at c. 310–320 Ma (Ewing et al. 2013; Williams et al. 2022; Wyatt et al. 2022) and was followed by an extended period (> 40 Ma) of HT conditions (Vavra et al. 1999; Ewing et al. 2013; Kunz et al. 2018). The HT to UHT metamorphism was accompanied by widespread anatexis and formation of metatexite to diatexite migmatites (e.g., Schnetger 1994; Barboza and Bergantz 2000; Barboza et al. 1999; Redler et al. 2012, 2013; Kunz et al. 2014; Carvalho et al. 2019, 2020; Bartoli and Carvalho 2021; Kunz and White 2019).

After the post-orogenic extension during the Permian, the IVZ experienced multiple episodes of rifting during the Triassic-Jurassic (e.g., Henk et al. 1997; Rutter et al. 2007; Smye et al. 2019). Crustal thinning was accommodated by several shear zones (e.g., Brodie et al. 1987; Siegesmund et al. 2008; Corvò et al. 2022; Simonetti et al. 2023).

Field and petrographic features of metapelitic, metapsammitic and metabasic rocks from Val Strona di Omegna have been extensively described in several papers –among the others Bertolani (1964a, b, c) Bertolani (1968); Bertolani and Rivalenti (1966); Zingg (1980); Redler et al. (2012,

Fig. 5 (**a**) Schematic map of Val Strona di Omegna, redrawn after Redler et al. (2012). Colored stars mark the position of rock samples for which temperature estimates were calculated (literature data from: Henk et al. 1997; Bea and Montero 1999; Luvizotto and Zack 2009; Redler et al. 2012; Ewing et al. 2013; Kunz et al. 2018; Kunz and White 2019; Wyatt et al. 2022). FRSZ: Forno-Rosarolo shear zone (from Simonetti et al. 2023) (**b**) Metamorphic field gradient for Val Strona di Omegna (KW19) based on peak mineral assemblage fields from metabasic and metapelitic rocks (redrawn from Kunz and White 2019)

2013); Kunz et al. (2014); Kunz and White (2019); Carvalho et al. (2019, 2020, 2023a); Simonetti et al. (2023), to which the interested reader is referred. In this study, seven metabasic rocks were collected for the application of Ti-in-amphibole thermometer (STR105 and STR133 from amphibolite facies zone, STR82, STR86 and STR116 from transition zone, STR130 and STR120 from granulite facies zone; Fig. 5a) and are briefly described below. Metabasites from Val Strona di Omegna were interpreted as former basalt injections into an accretionary sedimentary wedge (Sills and Tarney 1984; Mazzuchelli and Siena 1986) and were geochemically classified as N-MORB and E-MORB.

Field relationships and petrography

Samples STR105 and STR133 were collected in the amphibolite facies zone; they are fine-grained, weakly foliated rocks (Fig. 6a), where the foliation is mostly defined by amphibole and, to a lesser extent, by intergrowths of biotite and amphibole. The mineral assemblage is composed of green hornblende, plagioclase, quartz and biotite (Fig. 7a, b). Rock STR133 also contains garnet crystals with mineral inclusions of amphibole, plagioclase and quartz. Accessory minerals include titanite, ilmenite, zircon, apatite and pyrite. These samples lack field evidence and microstructures indicative of partial melting.

In the field, rocks from the transition zone (STR116, STR82 and STR86) are characterized by the appearance of elongated (few centimeters long) patches of leucosome, subparallel to the foliation, containing quartz, plagioclase and pale green peritectic clinopyroxene (Fig. 6b, c). The latter often shows rational crystal faces against the leucocratic matrix (Fig. 6c), suggesting its formation in the presence of melt (Sawyer 2008). The mineral assemblage is composed of hornblende (mostly green and brown in STR116 and STR86, respectively), clinopyroxene, plagioclase and quartz with rare biotite (Fig. 7c, d). Accessory minerals are ilmenite, zircon and apatite. In places, mafic selvedges composed of coarse-grained amphibole develop around leucocratic patches (Fig. 6b, d, and 7d-f). In sample STR82, plagioclase, and clinopyroxene in leucosome are often partially altered and replaced by fine-grained mineral aggregates (Fig. 7d-f), whereas the selvedge-forming amphibole
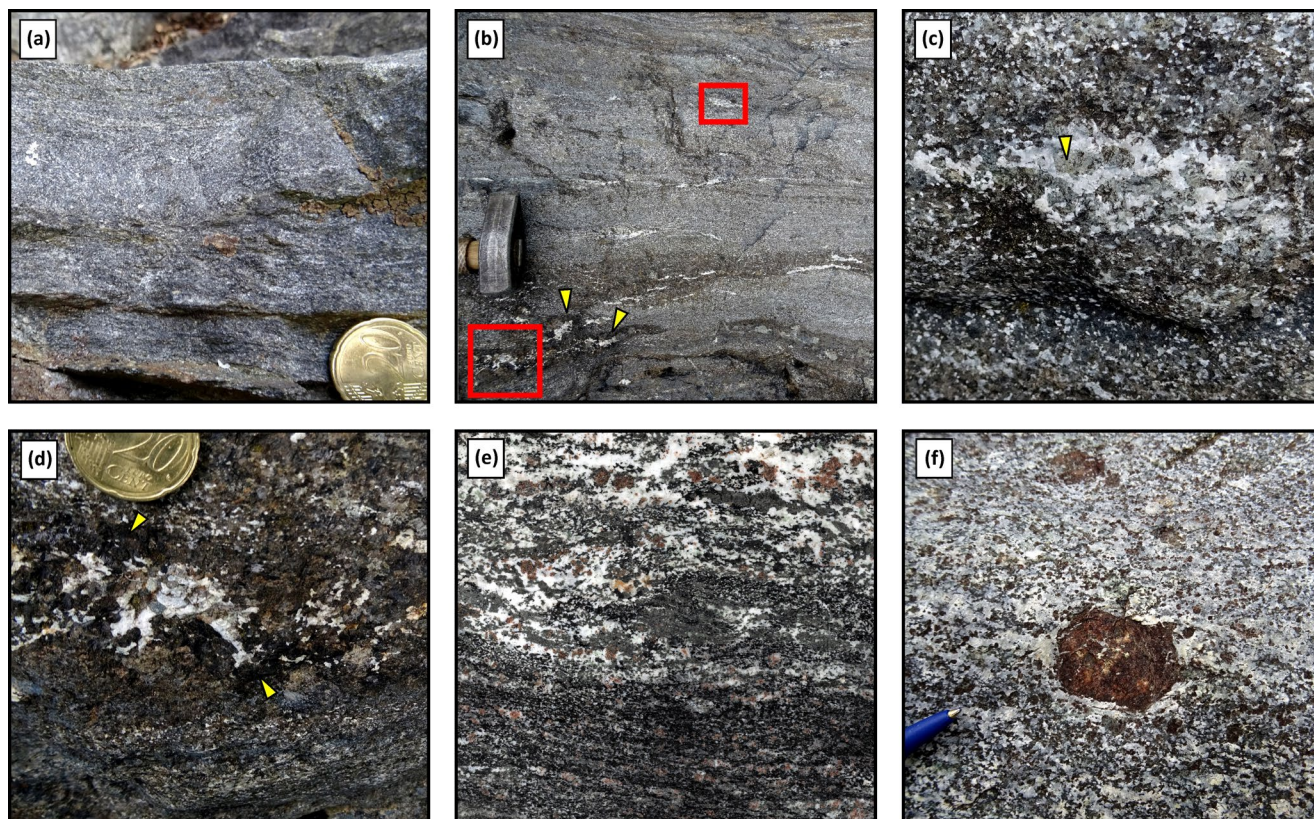

Fig. 6 Field aspect of metabasic rocks from the Kinzigite Formation, Val Strona di Omegna. (**a**) Fine-grained metabasic rock STR105 from the amphibolite facies zone. (**b**) Partially-melted amphibolite STR82 from the transition zone showing segregation of patchy leucosomes. Mafic selvedges of amphibole can be present at the contact between the leucosome and the matrix (yellow arrows). (**c**) Close-up of (**b**), showing a patchy leucosome made of pale green clinopyroxene (yellow arrow), quartz and plagioclase. (**d**) Close-up of (**b**), showing amphibole-rich mafic selvedges (yellow arrows) around leucosome segregation. The size of amphibole clearly decreases from the selvedge to the matrix. (**e-f**) Granulite facies metabasic rocks STR130 and STR120, respectively, ranging from metatexite (**e**) to diatexite (**f**)
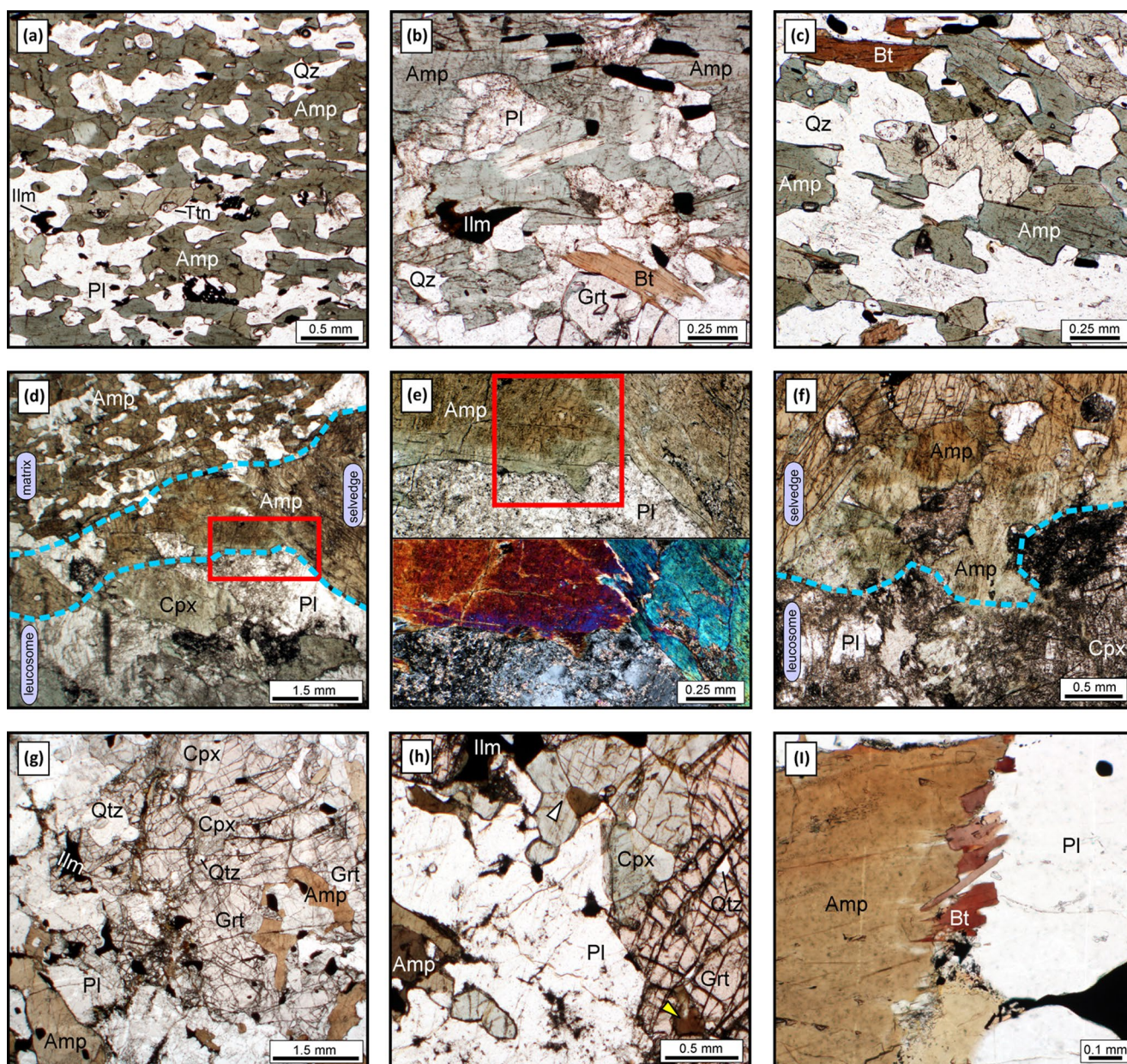
Fig. 7 Photomicrographs of metabasic rocks from the Kinzigite Formation, Val Strona di Omegna. (**a,b**) Amphibolite facies samples STR105 and STR133 containing lepidoblastic amphibole. (**c**) Sample STR116 from the transition zone with the mineral assemblage amphibole, biotite, quartz, plagioclase and ilmenite. (**d**) Sample STR82 from the transition zone where mafic selvedges composed of coarse-grained amphibole were developed at the contact between leucosome and the rock matrix (area bounded by dashed light blue lines). The leucosome is composed of coarse-grained quartz, plagioclase and clinopyroxene. Red area: figure (**e**). (**e**) Close-up of (**d**) showing the transition from brown to green amphibole at the contact with leucosome; plagioclase is strongly altered. Plane polarized light (upper portion) and crossed polars (lower portion). Red square: area of Fig. 11. (**f**) Brown to green amphibole in a mafic selvedge of STR82; plagioclase and clinopyroxene from leucosome are strongly altered. Dashed light blue line: boundary between mafic seldvedge and leucosome (**g, h**) Mafic granulites STR130 and STR120 with the mineral assemblage amphibole, garnet, clinopyroxene, orthopyroxene, quartz and ilmenite; yellow arrows: inclusion of amphibole in garnet; white arrow: triple junction between two clinopyroxene crystals and amphibole. (**i**) Biotite overgrowths replacing amphibole rim; sample STR130

shows a change in color from brown to green towards the contact with leucosome (Fig. 7e, f).

Rocks from granulite facies zone (STR130 and STR120) are granoblastic with evident millimeter- to centimeter-sized porphyroblasts of garnet, clinopyroxene and orthopyroxene (Fig. 6e, f). The mineral assemblage also contains hornblende, plagioclase, quartz, minor biotite and accessory ilmenite, apatite and pyrite. Last remnants of hornblende

occur included in garnet along with quartz or are scattered in the matrix (Fig. 7g, h); in the latter textural setting, amphibole rim is often overgrown by tiny (0.1–0.2 mm) biotite crystals (Fig. 7i).

Methods

Major element compositions of amphibole were analysed using a JEOL JXA 8200 Superprobe at the Dipartimento di Scienze della Terra, Università di Milano, Italy. The operating conditions for WDS were 5 nA beam current, 15 kV accelerating voltage, counting time of 30s on peak and 10s on background. Natural minerals and synthetic oxides used for calibration are: omphacite (Na), grossular (Al, Si, Ca), fayalite (Fe), rodonite (Mn), K-feldspar (K), olivine (Mg), ilmenite (Ti), scapolite (Cl), Cr_2O_3 (Cr). Detection limits (1s) were ca. 0.01 wt% for Al, K and Ca, 0.02 wt% for Mg, Si, Na and Cl, 0.03 wt% for Cr, Fe, Ti, Mn. Ti measurements have a precision between ± 8–16% (2σ). Backscattered electron imaging (BSE) and X-ray elemental maps were obtained with a TESCAN SOLARIS dual beam FIB-FE-SEM available at the Dipartimento di Geoscienze, Università di Padova, Italy. Chemical maps were obtained with the Ultim max 65 Oxford Instrument silicon drift EDS, at working conditions of: 10 nA beam current, 15 kV acceleration voltage and 1 μm beam diameter. The amphibole formulas were calculated using the spreadsheets available in Ridolfi et al. (2018), on the basis of 23 oxygens.

Rock samples were crushed and then powdered in a tungsten ring mill. The major element composition of the samples was obtained by X-ray fluorescence (XRF) with a Panalytical Zetium spectrometer at the Dipartimento di Geoscienze, Università di Padova, using international rock standards (Govindaraju 1994). Absolute uncertainties in XRF analyses are in the range of 0.5 wt% (2σ) for major elements such as SiO_2 to < 0.01 wt% for minor elements.

Results

Bulk rock composition

Investigated rocks show SiO_2 contents ranging between 44 and 51 wt% and $Na_2O + K_2O$ between 1.3 and 3.8 wt%, belonging to the subalkaline series, with Mg# between 0.3 and 0.5 (Table S1). In the ACF compatibility diagram, they plot in the field of common mafic rocks (Fig. S1). Bulk rock compositions are variable and no systematic trends were observed in major elements across the Kinzigite Formation, except for SiO_2 which decreases with increasing metamorphic grade (Fig. S2). TiO_2 varies between 1.00 and 3.31

wt%, with sample STR82 showing the lowest TiO_2 content (1.00 wt%), while other samples from the transition zone have TiO_2 between 2.5 and 2.8 wt%. In terms of trace elements, sample STR82 is strongly depleted in Zr (56 ppm) compared to other metabasites (150–289 ppm). Ni and Cr contents are much higher in STR116 and STR82 (217–256 ppm and 490–578 ppm, respectively) than the other samples (24–65 ppm and 17–74 ppm, respectively).

Amphibole composition

A total of 358 analyses of amphibole were obtained from the seven selected samples and they are listed in supplementary Table S2. All analyzed grains are classified as calcium amphibole, with Si = 6.1–7.8 apfu, Ca = 0.9–2.0 apfu and Mg# = 0.41–0.76 and are plotted in Fig. 8. A compositional variation is observed across the crustal sequence, with magnesio-hornblende typical in amphibolite facies rocks, magnesio-hornblende to pargasite in the transition zone and pargasite to sadanagaite in granulite facies zone (Fig. 8a). Analyses from each sample are clustered together, with the exception of rock STR82 where the composition of amphibole spreads out over a wide range, pointing toward the tremolite-hornblende boundary (Fig. 8a). Importantly, amphiboles from amphibolite facies rocks have a lower occupancy of the A-site compared to those from other samples. Consequently, they define a different trajectory in the compositional space of Fig. 8a.

In the dataset, the TiO_2 content ranges from 0.14 to 3.76 wt% (Ti = 0.015–0.426 apfu) and increases with increasing metamorphic grade (Figs. 8b and 9). The highest Ti values in each sample increases from amphibolite (0.125–0.147 apfu), to transition (0.152–0.210 apfu), up to granulite facies (0.393–0.426 apfu) (Fig. 9). The lowest Ti contents are found in samples STR133 and STR82 from amphibolite facies and transition zones, respectively. The lowest Ti values found in granulites overlap with the highest ones in transition zone rocks (Figs. 8b and 9). Liao et al. (2021) proposed to utilize the diagram Si vs. Ti to roughly discriminate metamorphic facies on the basis of amphibole composition. Adopting their compositional fields for the high amphibolite facies (HAM) and the granulite to ultrahigh granulite facies (HT-GR and UHT), respectively, amphiboles from STR105, STR133 and STR82 plot within the HAM field, the majority of those from STR120 and STR130 in the UHT field, whereas those from STR86 within the overlapping area between HAM and HT-GR (Fig. 8b). The analyzed grains from rock STR116, instead, straddle the boundaries between HT-GR and HAM amphiboles.

All the analyzed amphiboles display a distinct positive correlation between Na and K content on the A-site [$(Na + K)^A$] and tetrahedral Al, indicating edenite substitution (Fig. 10a).
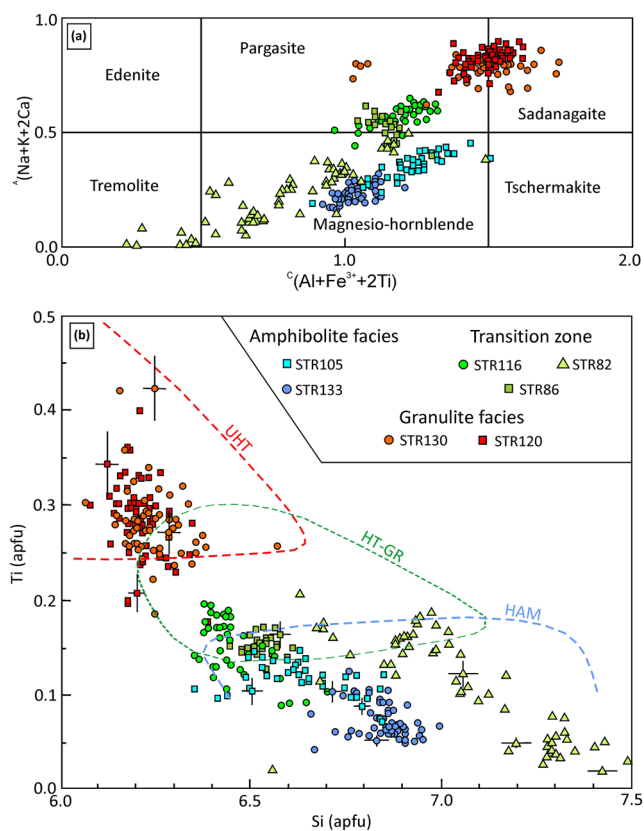
Fig. 8 (**a**) Classification of calcium amphibole from the investigated rocks, based on Hawthorne et al. (2012). (**b**) Si vs. Ti diagram of studied amphiboles with the boundaries for high amphibolite facies (HAM), high-temperature granulite facies (HT-GR) and ultrahigh temperature granulite facies (UHT) proposed by Liao et al. (2021). The temperatures inferred for HAM, HT-GR and UHT fields are 680–800, 800–900 and > 900 °C, respectively (more details in Liao et al. 2021). Analytical uncertainties (2σ) related to the counting statistics were propagated through the mineral recalculation following De Angelis et al. (2013) and are reported for some representative analyses (black bars). The uncertainty is smaller than the symbol for the lowest Ti contents

Overall, the Ti concentrations increase with increasing Al^{IV}, which could indicate the operation of the Ti–Tschermak substitution (Fig. 10b). However, an exception to this general behavior is represented by the amphiboles from granulites, where the Ti content varies between 0.2 and 0.4 apfu at constant values of Al^{IV} (ca. 1.75 apfu). Additionally, in this plot STR82 clearly defines a separate trend with respect to other rocks. In the Al^{IV}-Al^{VI} plot of Fig. 10c, amphiboles from rocks STR82 and STR105 define a positive linear trend, which indicates Al–Tschermak substitution in these samples.

The internal variability of Ti in amphibole from individual rock samples varies from small (ΔTi = 0.045 apfu; STR86) to large (ΔTi = 0.082 and 0.142 apfu; STR133 and STR82) (Fig. 9). In granulite samples, the Ti concentrations varies with the textural position, with amphibole rims that

generally show lower Ti values when overgrown by Ti-rich biotite (TiO_2 = 4.7–5.2 wt%) (Fig. 9). In sample STR82, Ti systematically decreases from core of matrix grains to selvedge-forming amphiboles, with the lowest values found approaching the selvedge-leucosome boundary (Fig. 9). This is evident in the X-ray elemental maps reported in Fig. 11, documenting a sharp compositional variation between amphibole interior and rim. The latter is depleted in Ti, Al, K and Na, and enriched in Mg and Si when in contact with altered leucosome.

Ti-in-amphibole temperatures

The temperature recorded by amphibole in each sample has been calculated applying the equation proposed by Liao et al. (2021) and the estimates are reported in Table S2. In all the investigated rocks, amphibole coexists with a Ti-phase (titanite and/or ilmenite) randomly distributed across the sample, whose presence is critical to obtain reliable temperature using this thermometer. Titanium measurements have a precision of ± 8–16% (2σ), which contributes an additional uncertainty of ± 5–30 °C over the compositional range investigated in this study.

The average temperatures in each sample range from 632 to 706 °C (amphibolite facies), 655 to 773 °C (transition) and 885 to 890 °C (granulite-facies) (Fig. 9). The widest temperature variability is observed in rock STR82 from the transition zone.

When the textural setting of the amphibole is considered for this sample, three temperature peaks are observed: ≈ 770 °C (average temperature) for amphibole in the matrix, ≈ 710 °C for amphibole forming mafic selvedges and ≈ 525 °C for portions of amphibole in mafic selvedges at the very contact with leucosome (Fig. 9). In the latter textural setting, the lowest Ti content of 0.015 apfu corresponds to a temperature of ≈ 450 °C (Figs. 9 and 11). In granulites, similar average temperatures of ≈ 900 °C are obtained from the two investigated samples; when amphibole rim is overgrown by biotite, the calculated temperatures decrease to ≈ 830 °C (the lowest temperature value is 785 °C) (Fig. 9).

Discussion

Conventional thermobarometry, phase equilibria modelling and quadrivalent (4+) cation thermometry have been all applied along the continuous metamorphic field gradient exposed in Val Strona di Omegna over the last 40 years (e.g., Henk et al. 1997; Bea and Montero 1999; Redler et al. 2012; Ewing et al. 2013; Kunz et al. 2018; Luvizotto and Zack 2009; Kunz and White 2019). In this study, we firstly focus on the significance (i) of the Ti contents measured in

Fig. 9 Box and whisker plots of the Ti content of amphibole and calculated temperatures for metabasites across the Val Strona di Omegna. Data were grouped on the basis of their textural setting; Rim(Bt): amphibole rim characterized by the presence of biotite overgrowths; selv./ leucos.: rim of selvedge-forming amphibole at the contact with leucosome. Black vertical bars show the error (2σ) inherent in the calibration at 600 and 900 °C, respectively
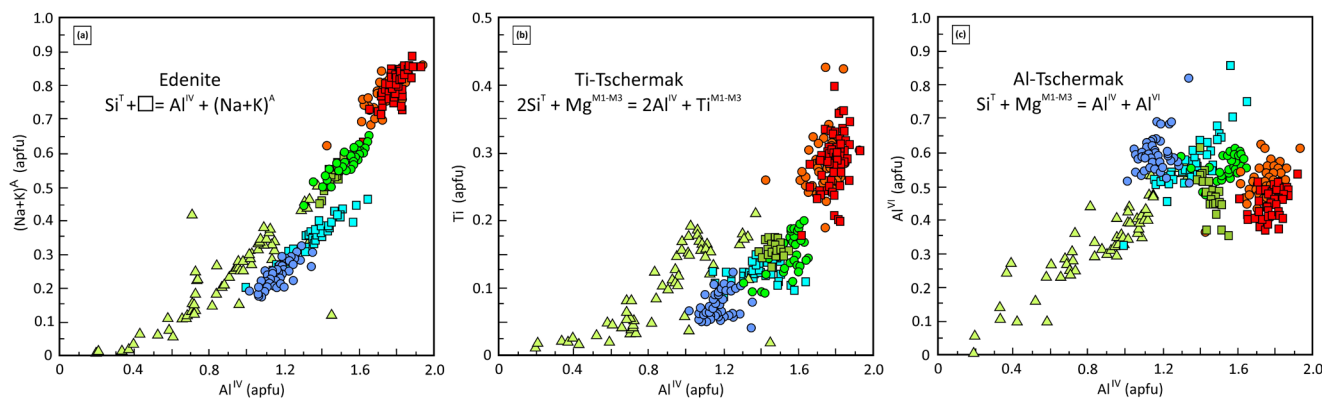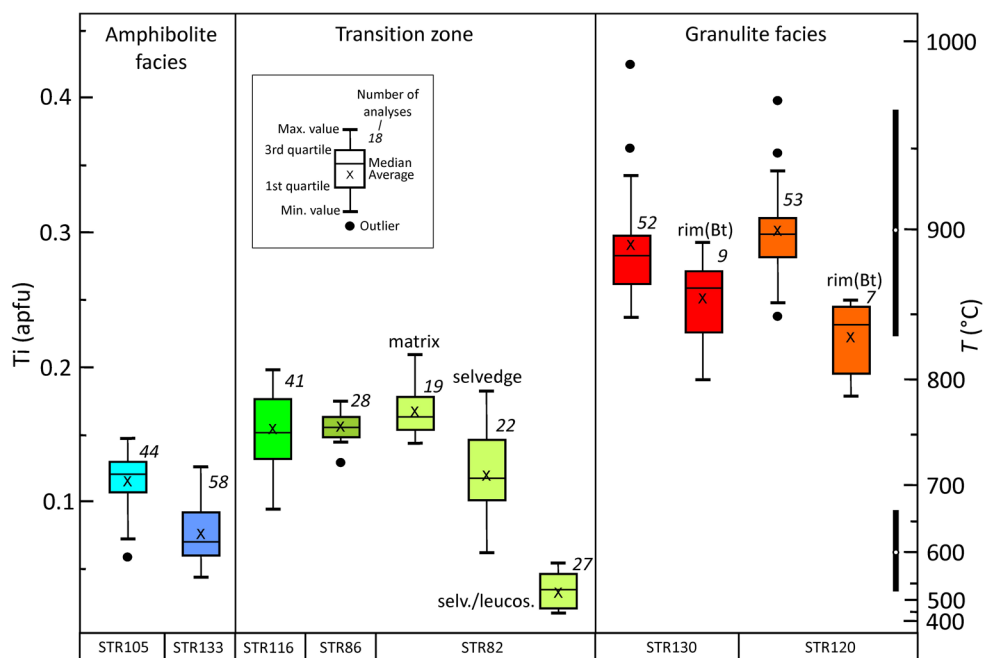

Fig. 10 Compositional variation in amphiboles. (**a**) A-site occupancy vs. tetrahedral aluminum (Al^{IV}). (**b**) titanium vs. Al^{IV}. (**c**) octahedral aluminum (Al^{VI}) vs. Al^{IV}. Symbols as in Fig. 8

amphibole from IVZ metabasic rocks and (ii) of the temperatures obtained by Ti-in-amphibole thermometry. Secondly, we use all the thermometric constraints available from the Val Strona di Omegna to compare how the different thermometers perform across this crustal section, focusing in particular on granulite facies rocks. We then focus on other UHT terranes to better understand the fidelity of Ti-in-amphibole thermometry under extreme crustal conditions. Lastly, potential implications for Ti diffusivity in amphibole are discussed.

Significance of Ti content of amphibole and calculated temperatures

The positive correlation observed for amphibole composition in Ti vs. Al^{IV} and $(Na+K)^A$ vs. Al^{IV} plots and the increase

of these compositional values with increasing metamorphic grade (Fig. 10a, b) are consistent with the well-known effect of temperature on the Ti-Tschermak and edenite exchange vectors (e.g., Spear 1981; Holland and Blundy 1994). Additional substitution occurs in samples STR82 and STR105 via Al-Tschermak exchange vector (Fig. 10c), which is pressure-dependent (Hollister et al. 1987; Thomas and Ernst 1990; Schmidt 1992). However, another substitution mechanism appears to play a role in the HT amphiboles. This is the Ti-oxy substitution, in which the dehydrogenation is accompanied by substitution of one divalent cation in the $M(1)$ site by Ti^{4+} (King et al. 1999). This exchange mechanism would explain the lack of a clear correlation between Ti and Al^{IV} in amphibole from granulites (Fig. 10b). However, a more precise assessment of the importance of the
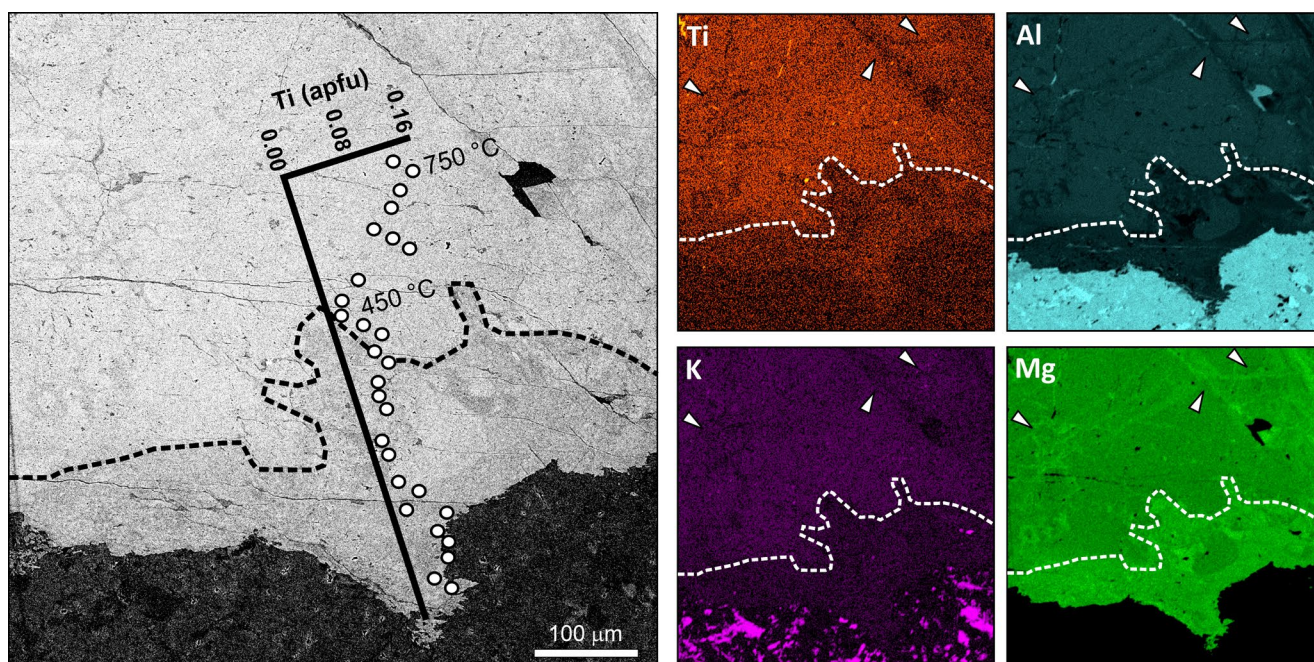
Fig. 11 BSE image and elemental EDS X-ray maps of amphibole from a mafic selvedge of sample STR82. The investigated area is represented by a red square in Fig. 7e. The portion of amphibole in contact with the leucosome is depleted in Ti, K, Al and Na (not shown), and enriched in Mg and Si (not shown). Similar compositional variations occur also in the grain interior and are associated to the presence of fractures (white arrows). A quantitative EMP concentration profile of Ti is reported on the BSE image together with the Ti-in-amphibole temperatures calculated for the highest and lowest Ti contents, respectively

Ti-Tschermak and Ti-oxy substitutions requires direct measurements of H and Fe^{3+} contents in amphibole.

Composition of calcic amphibole is sensitive to temperature, pressure, fO_2 and bulk composition. To evaluate the control exerted by the composition of the bulk system, amphibole compositions are compared with the composition of host rocks (Fig. 12). Notably, the composition of amphibole from rock STR82 is markedly different from that of amphiboles from the other rocks in the transition zone (i.e. STR116 and STR86), with the former showing the highest Mg# and the lowest Al_2O_3 and $Na_2O + K_2O$ values (Fig. 12). These chemical features are partially controlled by the composition of the bulk rocks. In fact, sample STR82 shows the highest Mg# and CaO content of the dataset, but its Al_2O_3 content is similar to the values exhibited by the other rocks. Regarding TiO_2, rock STR82 shows the lowest content, a feature that is reflected by the composition of some of their amphiboles having $TiO_2 < 0.5$ wt%. (Fig. 12). However, no systematic trends between rock and amphibole compositions are recognizable for Ti in all the other samples. For instance, amphiboles from granulites STR130 and STR120 show similar TiO_2 contents, despite a markedly different bulk rock composition (3.3 vs. 1.6 wt% TiO_2, respectively) (Fig. 12). The Ti content of amphibole seems to be mainly buffered by the presence of a Ti-phase (ilmenite, rutile, titanite), even though a control of the bulk rock

TiO_2 content cannot be excluded for amphibole grains from rock STR82 (Fig. 12).

The application of the Ti-in-amphibole thermometry in this study shows increasing temperatures matching the increasing metamorphic grade (Fig. 9). The highest temperatures (850–980 °C; average ≈ 900 °C) for granulites are those calculated for amphibole from the rock matrix and for grains included in garnet (Fig. 7). Much lower temperatures (average ≈ 830 °C, but up to 785 °C) are instead recorded by amphibole rims overgrown by small Ti-rich ($TiO_2 = 4.7–5.2$ wt%) biotite crystals (Fig. 9). Since these microstructures are the result of retrograde reactions, the temperature range of ≈ 785–850 °C suggests that resetting of the Ti-in-amphibole thermometer likely occurred in the presence of melt, as supported by field and petrographic observations (see above). Therefore, the newly formed biotite can be interpreted as product of retrograde reactions between residual amphibole and anatectic melt, where the former provided Fe, Mg and Ti and the latter K. Although leucosomes in metabasites are dominated by quartz, plagioclase and clinopyroxene, reflecting a K-poor tonalitic composition, the injection of K-bearing leucosomes from the adjacent metapelites has been well documented in IVZ metabasites (Harlov and Förster 2002; Kunz et al. 2014).

The three samples from the transition zone mostly yielded temperatures between ≈ 740 and ≈ 800 °C (Fig. 9), even though the widest temperature range (≈ 300 °C) of the

Fig. 12 Compositional variations of amphiboles and bulk rocks. Small symbols as in Fig. 8b
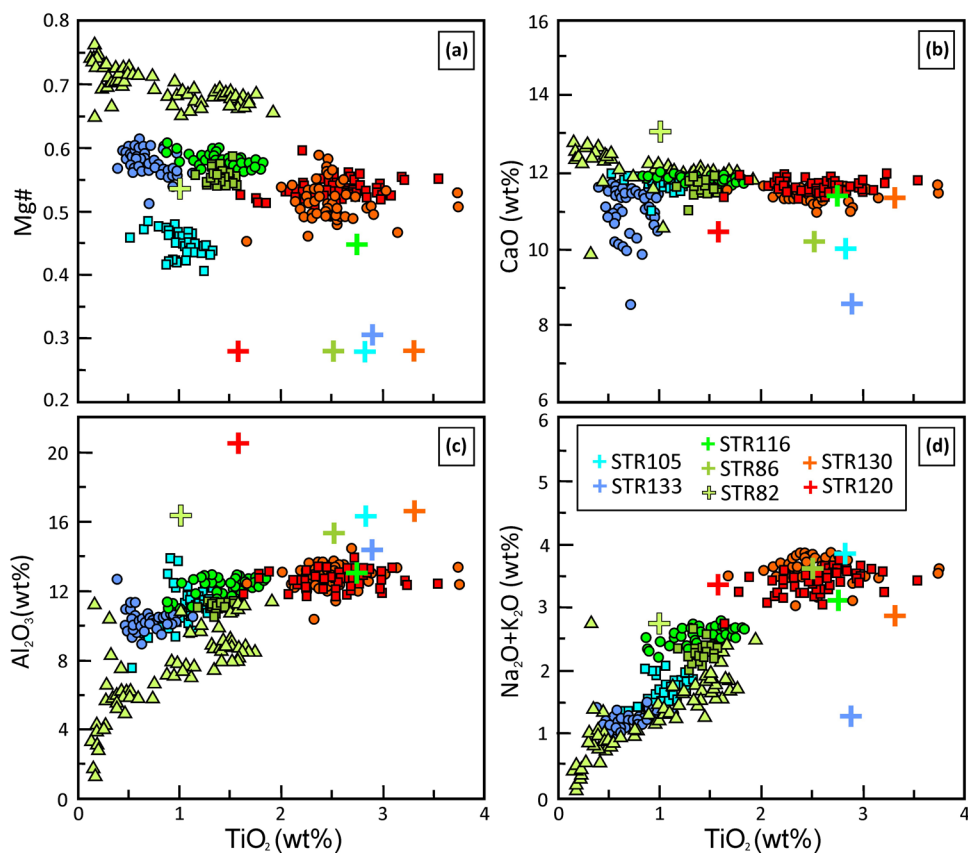
dataset presented in this study was found in sample STR82. This sample also records the lowest temperature of this crustal section (≈ 450 °C). Temperatures from amphibole core in the matrix of STR82 (≈ 760–810 °C) are likely to be related to the prograde to peak evolution, being similar to those documented in the nearby sample STR86 (Fig. 9).

Amphibole-rich selvedges in mafic migmatites are interpreted to form by reaction between a leucosome and its wallrocks during melt crystallization, similar to the biotite-rich ones in metapelitic migmatites (Sawyer 2008). Temperatures of 680–750 °C provided by amphibole in the selvedge (Fig. 9) would be consistent with such a process occurring in the presence of melt. However, the portions of amphibole grains directly in contact with leucosome are commonly depleted in Ti and provide much lower temperatures (≈ 450–600 °C; Figs. 9 and 11), which are not consistent with suprasolidus conditions. It should be noted that (i) these temperatures are lower than those for which the Ti-in-amphibole thermometer was calibrated (≥ 700 °C) and (ii) we do not know if this portion of amphibole was in equilibrium with a Ti-saturating phase during its formation/modification. Although caution should be used when interpreting these temperature values, the detailed microstructural and microchemical characterization clearly indicates

that amphibole composition has been modified (Figs. 7d-f, 9 and 11).

Leucosome in sample STR82 shows clear evidence of hydration after crystallization, with retrograde fine-grained sericite and chlorite replacing plagioclase and clinopyroxene, respectively (Figs. 7d-f and 11). Several lines of evidence testify for retrograde fluid influx across IVZ crustal section (e.g., Boriani and Villa 1997; Vavra et al. 1999; Franz and Harlov 1998; Luvizotto and Zack 2009; Ewing et al. 2013; Smye et al. 2019) and the origin of these fluids has been ascribed to the Permian post-magmatic exsolution following the crystallization of the Mafic Complex (e.g., Ewing et al. 2013) and/or to the Triassic to Jurassic lithospheric thinning and rifting (e.g., Ewing et al. 2015; Langone et al. 2017; Smye et al. 2019). Interestingly, Smye et al. (2019) argued that IVZ underwent local fluid infiltration when temperature was ≈ 500 °C during Tethyan extension. Such subsolidus temperatures are consistent with the ones reported by sample STR82 in this study.

The compositional change toward the rim of amphibole in the selvedge is quite sharp and did not occur steadily (Fig. 11). Moreover, a similar depletion in Ti, K and Al is also present in amphibole interior in the form of crosscutting veins (white arrows in Fig. 11). These textures exclude the possibility of Ti diffusion out of amphibole during

cooling. Rather, we interpret the composition of amphibole rim in contact with altered leucosome of rock STR82 to have been modified by fluid-rock interaction. Fluid percolation was mostly confined within near-leucosome portions probably due to the larger grain size compared to the surrounding matrix (Figs. 6c and 7d), which enhances porosity. Moreover, self-generated transient fluid pathways are likely to form in feldspar-rich portions of rocks undergoing fluid-mediated alteration, enhancing mineral transformation reactions (Plumper et al. 2017).

Textures associated to rutile replacement in IVZ metapelites are considered to support that Ti and Zr, frequently interpreted to be immobile elements, can be significantly mobilized by hot fluids (Luvizotto and Zack 2009; and discussion therein). Our results indicate that Ti mobilization was not solely confined to metapelites, but it likely involved other lithologies. Noteworthy, Harlov et al. (2006) documented newly-formed titanite rims in metabasites of Val Strona di Omegna, interpreted as result of fluid-assisted mass transport. Bulk rock analyses support this view, as rock STR82 shows much lower contents of TiO_2 and Zr compared to other metabasites (Table S1).

Performance of different thermometers across the central Ivrea–Verbano Zone

Figure 13a shows a comparison between published thermometric constraints from metapelites, metagreywackes and metabasites across the section of Val Strona di Omegna with Ti-in-amphibole temperatures presented in this study. Temperatures provided by each sample are plotted as a function of metamorphic grade, against distance from the Insubric Line. Rutile temperatures have been recalculated using the equation recently proposed by Kohn (2020) and the Zr contents reported by Luvizotto and Zack (2009) and Ewing et al. (2013). To avoid the strong resetting of the Zr content, Luvizotto and Zack (2009) suggested to select exclusively values above the 90th percentile in each sample. We followed this suggestion and considered lower values as reset temperatures (dashed portion of red bars in Fig. 13a). Similarly, temperature values provided by Ti-in-amphibole thermometry for selvedge-forming amphibole in sample STR82 and for amphibole rims in contact with retrograde biotite in granulites STR130 and STR120 are not considered.
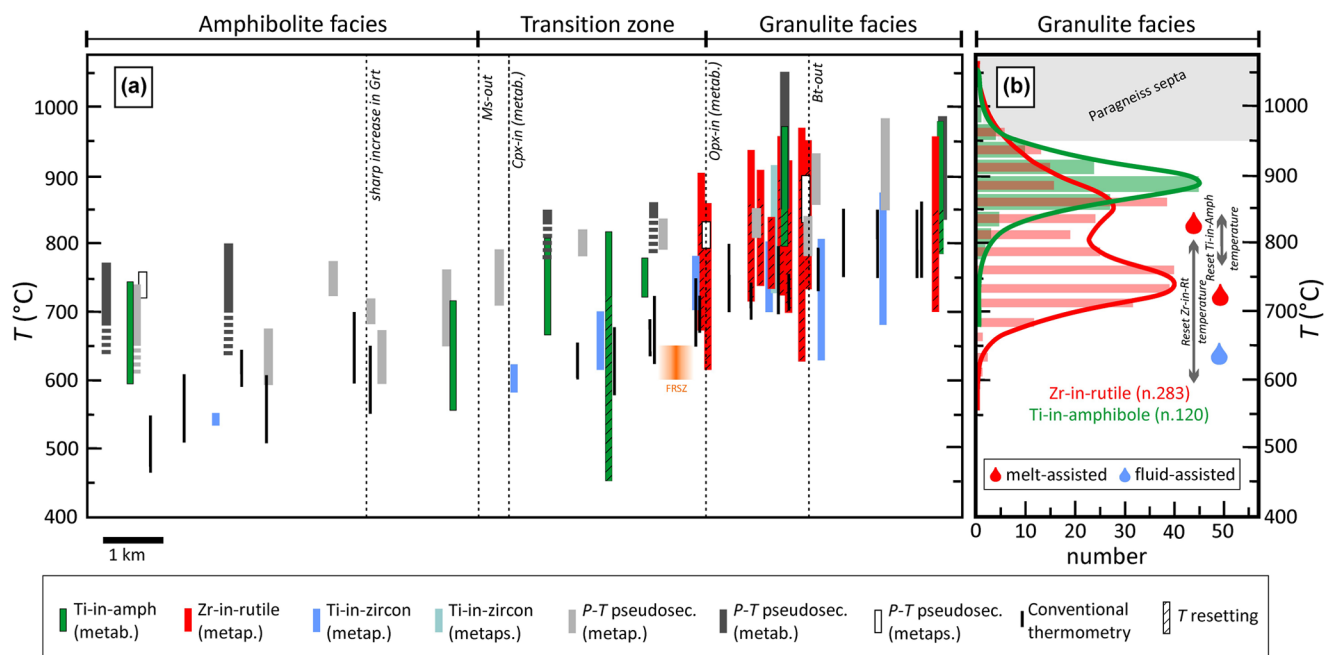

Fig. 13 (a) Temperature constraints obtained from different thermometers across the IVZ crustal sequence. Location of samples was projected onto a linear transect of Val Strona di Omegna. Conventional thermometry is from Henk et al. (1997) and Bea and Montero (1999). P–T pseudosection constraints are from Redler et al. (2012), Kunz and White (2019) and Wyatt et al. (2022). Rutile data are from Luvizotto and Zack (2009) and Ewing et al. (2013), recalculated considering the equation proposed by Kohn (2020); a pressure of 8 kbar was commonly used, with the exception of the highest-grade sample (9 kbar). Ti-in-zircon temperatures are from Ewing et al. (2013) and Kunz et al. (2018). FRSZ: Forno-Rosarolo shear zone (temperature estimates from Simonetti et al. 2023). Amphibole thermometry is from this study. Dashed lines correspond to the in-field location of the extrapolated mineral isograds (from Redler et al. 2012). The hatched area in colored bars reflects cooling or reset temperatures recorded in rutile and amphibole grains. Hatch lines below some vertical bars reflect extension to lower temperatures due to the mismatch between textural observations and phase equilibria modeling. (b) Histograms showing frequencies of temperature estimates obtained by Ti-in-amphibole (green) and Zr-in-rutile (red) thermometers on mafic and pelitic IVZ granulites, respectively. Green and red curves reflect Kernel Density Estimation (KDE) of calculated temperatures. The grey area marks the temperature estimates obtained for metapelitic septa within the Mafic Complex (data from Ewing et al. 2013; Pape et al. 2016)

In comparing all temperature ranges reported in Fig. 13a, it is worth recalling that diverse thermometric techniques suffer from different uncertainties. The calibration uncertainties (2σ) for quadrivalent (4+) cation thermometry are usually < ± 30 °C, with the exception of Ti-in-amphibole thermometer (± 70 °C; Table 1). Regarding the error associated to analytical uncertainties, Ewing et al. (2013) reported values of ± 15–25 and ± 10–20 °C for Zr-in-rutile and Ti-in-zircon thermometers, respectively, applied to IVZ rocks. These uncertainties are similar to those calculated in this study considering the analytical error in the determination of Ti content in amphibole (± 5–30 °C; Table 1). Values of ± 50 °C are commonly reported as uncertainties associated to conventional thermometry and P–T pseudosections (Powell and Holland 2008; Green et al. 2016). For the latter, however, it should be noted that quantifying uncertainties is still a challenge due to the absence of reliable calculations dealing with error propagation through thermodynamic databases and models.

For IVZ granulites, Ti-in-amphibole thermometry yields peak temperatures from 850 to 980 °C ($\approx$ 900 °C on the average), matching those obtained from P–T pseudosections as well as the highest values provided by Zr-in-rutile thermometer (Fig. 13a). Temperatures > 1000 °C reported for a single mafic granulite on the basis of phase equilibria modelling (Kunz and White 2019) are not supported by other thermometric techniques (Fig. 13a).

Rutile in IVZ metapelites is expected to form at > 850 °C (see detailed modelling and discussion in Luvizotto and Zack 2009; Carvalho et al. 2023a). However, temperatures obtained by Zr-in-rutile thermometer across the entire granulite zone are in the range of 600 to 975 °C, significantly lower than temperatures provided by Ti-in-amphibole thermometry and phase equilibria modeling for granulite rocks (Fig. 13a). All the studies on IVZ rutile have reported

Table 1 Examples of uncertainties reported for single-mineral thermometers

Thermometer	Calibration uncertainty (2σ)	Analytical uncertainty (2σ)
Zr-in-rutile	±50 °C (1); ±20 °C (2); ±20–30 °C (4)*; ±10–15 °C (4)*; ±13–30 °C (5)	±5–20 °C (2); ±15–25 °C (3); ±20 °C (6)**
Ti-in-zircon	±10 °C (2); ±10–15 °C (5)	±5–20 °C (2); ±10–20 °C (3)
Ti-in-quartz	±7% (3)***	±10–20 °C (3); ±5–40 °C (7)
Ti-in-amphibole	±70 °C (8)	±5–30 °C (9)

*propagated calibration errors; **average analytical uncertainty reported for the entire dataset; ***reported by Ewing et al. (2013) as calibration error that can be calculated from the adjustable parameters of Thomas et al. (2010). Data from: (1) Zack et al. (2004); (2) Watson et al. (2006); (3) Ewing et al. (2013); (4) Kohn (2020); (5) Ferry and Watson (2007); (6) Qi et al. (2022); (7) Wark and Watson (2006); (8) Liao et al. (2021); (9) this study

microstructural evidence suggesting post-peak resetting of Zr concentrations (Luvizotto and Zack 2009; Ewing et al. 2013; Pape et al. 2016). Ewing et al. (2013) discussed in detail all the possible ways of modifying Zr concentrations of rutile and concluded that recrystallization (i.e., dissolution-reprecipitation) under retrograde conditions was the most likely process to explain resetting of the thermometer at $\approx$ 700–800 °C. These values match most of the temperatures of zircon crystallization from anatectic melt in pelitic granulite (Fig. 13a; see below), reinforcing the view that rutile partly recrystallized in the presence of melt at $\approx$ 700–800 °C (Fig. 13b). On the other hand, Luvizotto and Zack (2009) also documented rutile veinlets associated with textures suggesting post-peak influx of fluid in IVZ granulites. Therefore, the lowest (< 700 °C) Zr-in-rutile temperatures likely reflect late resetting of Zr content in rutile in the presence of a fluid phase rather than melt (Fig. 13b).

The lowest temperatures documented by Zr-in-rutile thermometry for IVZ granulites (650–750 °C) are also recorded by Ti-in-zircon thermometer (Fig. 13a). In the detailed study of Kunz et al. (2018) on IVZ zircons, these authors argued that CL-textures are in most cases not disturbed by fluid alteration and that the scatter observed in the Ti-in-zircon temperatures is likely to reflect different growth periods. This interpretation is reinforced by the Ti distribution within analyzed zircons in granulite with only a single data-point indicating a temperature < 670 °C (see Fig. 7b in Kunz et al. 2018). The absence of Ti-in-zircon temperatures which are as high as those recorded by Ti-in-amphibole and Zr-in-rutile thermometers ($\approx$ 900–980 °C) are most probably due to the fact that zircon only starts crystallizing at lower temperatures ($\approx$ 650–850 °C; Ewing et al. 2013; Klötzli et al. 2014). However, the lowest Ti-in-zircon temperatures from the amphibolite facies and transition zones ($\approx$ 550–650 °C) are incompatible with crystallization from a melt. Excluding a dissolution-reprecipitation process in the presence of a fluid phase on the basis of textures of investigated zircons, Kunz et al. (2018) consider these low temperature values as an artifact resulting from erroneously considering $a_{TiO2} = 1$ in the calculation of Ti-in-zircon temperatures in a sample containing no rutile.

In amphibolite and transition zones, Ti-in-amphibole thermometry yields temperature estimates that are consistent with those obtained by phase equilibria modelling (Fig. 13a). On the contrary, conventional thermometry based on Fe–Mg exchange thermometers (Bt-Grt and Grt-Opx pairs; Henk et al. 1997; Bea and Montero 1999) provided significantly lower temperatures than those yielded by other techniques for near peak conditions across the entire crustal sequence (Fig. 13a), as result of the retrograde resetting of mineral compositions during slow cooling (Frost and Chacko 1989; Pattison et al. 2003).

Effectiveness of Ti-in-amphibole thermometry in UHT rocks

Since thermometry is a crucial tool to identify the mechanisms which generate UHT metamorphism, the validation of any new thermometric technique at these extreme crustal conditions is of paramount importance. Clark et al. (2019) reported a comparative study among different thermometers applied to a single UHT metapelitic sample from the Rauer Group, East Antarctica. These authors concluded that the most reliable estimates of peak UHT temperature are provided by Al-in-orthopyroxene thermometry.

The present work is mostly focused on ilmenite-bearing metabasites and an important finding is that Ti-in-amphibole thermometer seems to be more robust in recording peak near-UHT conditions, compared to Zr-in-rutile thermometry applied to coexisting pelitic granulites (Fig. 13). Despite the fact that some mafic and pelitic samples were collected from the same outcrop (Fig. 5a), Zr-in-rutile thermometer in metapelite records lower temperatures and thus resulted to be more prone to post-peak resetting compared to Ti-in-amphibole thermometry in metabasite (Fig. 13a). This is evident from Fig. 13b, where Ti-in-amphibole temperatures collectively show a single peak at ≈ 900 °C, whereas Zr-in-rutile thermometer is characterized by a bimodal distribution of temperatures, with two well-defined peaks at ≈ 860 and ≈ 730 °C. Temperatures of 850–900 °C for IVZ granulites are consistent with the geological and petrological scenario of the crustal section of Val Strona di Omegna where these rocks are not in direct contact with the Mafic Complex (Figs. 4 and 5). When metapelite slices are instead intermingled with gabbro of the Mafic Complex (i.e., the metapelitic septa of Val Mastallone and Valsesia; Fig. 4), the recorded temperatures are higher (950–1150 °C; Fig. 13b).

The bimodality of Zr-in-rutile temperatures reported for IVZ rocks with a well-defined temperature mode around 700–800 °C (Fig. 13b; see also Ewing et al. 2013) has been documented in many UHT terranes worldwide (see compilation in Kelsey and Hand 2015; Harley 2021), suggesting that dissolution-reprecipitation of rutile in the presence of residual melt may be a common process in granulite. For instance, in rocks from the Lützow-Holm Complex (East Antarctica) Carvalho et al. (2023b) reported lower temperatures for rutile grains trapped and re-equilibrated within former melt inclusions; instead, UHT conditions are better recorded by rutile within garnet and in the rock matrix. Mitchell and Harley (2017) documented a complete resetting of Zr-in-rutile temperatures in UHT granulites from Napier Complex (Antarctica) to ≈ 600–750 °C. In this case, the dissolution of rutile and mobility of Zr were attributed to saline fluid infiltration. This reinforces the importance of having alternative techniques (such as Ti-in-amphibole

thermometer) to validate the achievement of extremely hot crustal conditions.

To better evaluate the effectiveness of Ti-in-amphibole thermometry at UHT, we compiled a dataset of amphibole analyses from four localities where UHT conditions were documented (Fig. 14): the Rauer Group in East Antarctica, the Madurai Block in southern India, the Highland Complex of Sri Lanka and the lower continental arc crust beneath the Northern Volcanic Zone in Colombia. The calculated temperatures for amphibole grains interpreted as part of peak mineral assemblage in metabasites were compared (i) with those recorded by Zr-in-rutile and/or Al-in-orthopyroxene thermometry in nearby UHT metapelites (Fig. 14a-c) or (ii) with results of elastic geothermobarometry and phase equilibria modelling from the same sample (Fig. 14d). This comparison supports what is already shown by the IVZ data: Ti-in-amphibole technique seems to be a more faithful recorder of UHT conditions compared to Zr-in-rutile thermometry from coexisting pelitic granulites. The latter may return significantly lower temperature estimates, up to ≈ 650 °C in granulites from Rauer Group, East Antarctica (Fig. 14a) and it is fundamental to use the least reset rutile Zr concentrations in order to constrain peak UHT conditions (Fig. 14a, b).

Whereas the good match between Al-in-orthopyroxene (in pelitic granulite) and Ti-in-amphibole temperatures is a further evidence of the robustness of the amphibole-based thermometric technique when applied to ilmenite-bearing metabasites, (Fig. 14a-c), the rutile-bearing HP granulite from the Northern Volcanic Zone in Colombia tells a different story (Fig. 14d). The sample 18XC10 from Gianola et al. (2023) represents the residuum after partial melting of mafic rocks and displays a well-equilibrated texture made of pargasitic amphibole, garnet and rutile. Peak temperature, constrained by phase equilibria modelling and elastic geothermobarometry of quartz and zircon inclusions in garnet, ranges between 950 and 1150 °C. However, Ti-in-amphibole thermometry yields systematically lower values (800–900 °C; Fig. 14d). When equation reported in Fig. 3c for rutile-bearing rocks is applied, temperatures increase up to 960 °C. This finding reinforces the view that the calibration of Liao et al. (2021) underestimates temperature for rocks equilibrated in the rutile stability field, whatever their H_2O content is (< 0.1 wt% for sample discussed in Fig. 14d).

Ti diffusion in amphibole: a matter for further investigations

The preservation of peak temperatures ≥ 900 °C in amphibole from slowly cooled rocks suggests that Ti content of amphibole may be resistant to post-peak diffusive re-equilibration. However, experimentally-derived Arrhenian
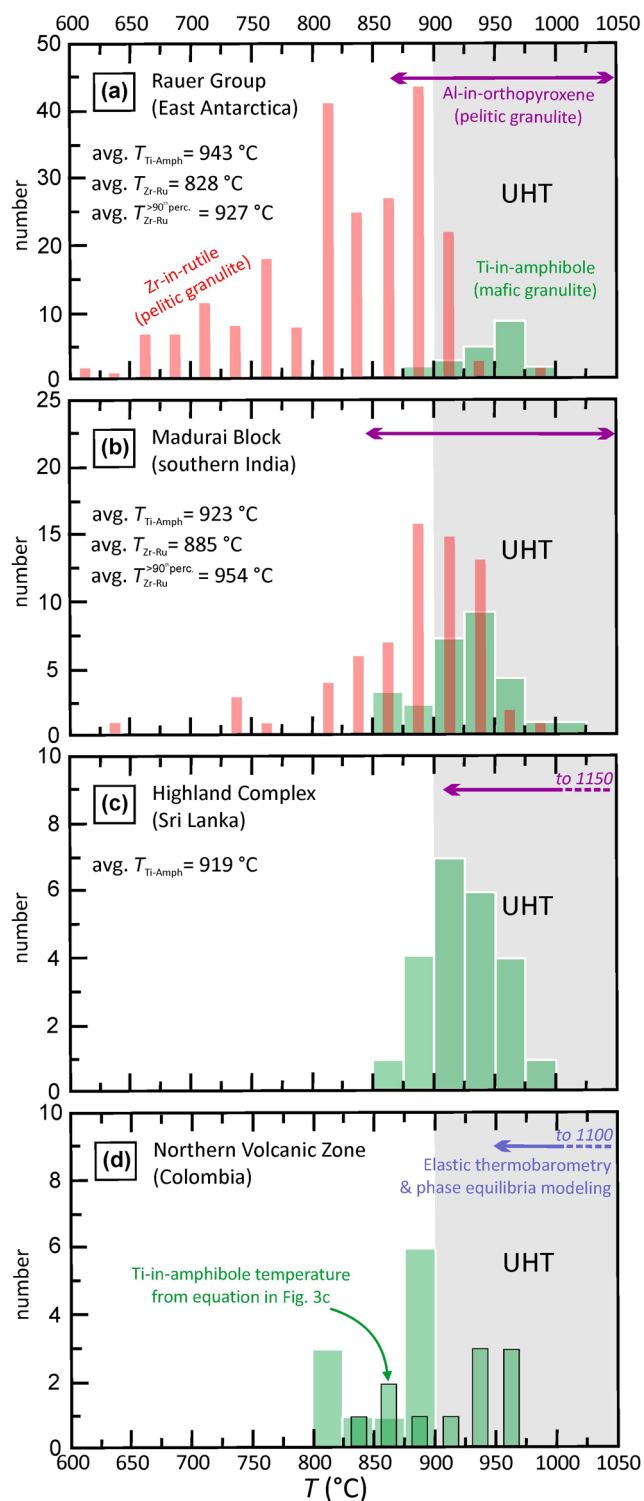
Fig. 14 Compilation of thermometric estimates from Rauer Group, East Antarctica (**a**), Madurai Block, southern India (**b**), Highland Complex, Sri Lanka (**c**) and Northern Volcanic Zone, Colombia (**d**). Ti-in-amphibole temperatures were obtained applying the calibration of Liao et al. (2021) and using amphibole compositions from the literature. Zr-in-rutile temperatures were recalculated considering the equation proposed by Kohn (2020) and Zr content of rutile and pressure values reported in the literature. The grey area marks the temperature field of UHT metamorphism. Average temperatures are reported for Ti-in-amphibole (Ti-Amph) and Zr-in-rutile (Zr-Ru) thermometers; for the latter, also average temperatures considering only values between the 90th percentile and the maximum are reported. Data from: Sajeev and Osanai (2004); Tamashiro et al. (2004); Sajeev et al. (2009); Prakash et al. (2010); Osanai et al. (2016); Hart et al. (2018); Clark et al. (2019); Dharmapriya et al. (2021); Dev et al. (2021); He et al. (2021); Ray et al. (2021); Shimizu and Tsunogae (2021); Chen et al. (2023); Gianola et al. (2023); Liu et al. (2023)

olivine (e.g. Cherniak and Liang 2012; Jollands et al. 2016; Cherniak and Watson 2020). Diffusivity values of Ti differ by more than three orders of magnitude (Fig. 15a). Jollands at al. (2020) highlighted the fact that a single element in a single mineral may have multiple diffusion mechanisms as a function of element concentration, and used this argument to explain the discrepancy of the Ti diffusivities in quartz reported in different studies.

We assume a simple model in which an amphibole grain with a radius x and a certain initial concentration is placed in a medium with a different concentration, driving diffusive loss from amphibole interior. Diffusion is considered to take place only in one dimension, perpendicular to the interface. Figure 15b reports the relation between diffusivity (D) and diffusion distance (x), calculated for different values of time (t), assuming the time-distance-diffusivity approximation $x \approx (Dt)^{1/2}$ (e.g., Watson 1982; Watson and Jurewicz 1984; Backer 1992; Acosta-Vigil et al. 2006). Considering that the high Ti contents measured in this study come from amphibole grains with a variable size from 200 μm to 1 mm, we assume a diffusion distance of 100 to 500 μm. After the thermal peak of 900 °C dated at ≈ 300–290 Ma, the IVZ experienced a protracted period of 20–30 Myr between 800 and 650 °C (Ewing et al. 2013, 2015). In order to preserve high Ti concentrations in the amphibole interior at these conditions, we calculated that the diffusivity (D) for Ti in amphibole must be slower than $10^{-21.5}$ and 10^{-23} m²sec⁻¹ for diffusion distances of 100 and 500 μm, respectively (Fig. 15b).

From this simplified model, it results that the diffusivity of Ti in amphibole at 650–800 °C might be similar to that in quartz (data from Jollands et al. 2020; Audétat et al. 2023), olivine and pyroxenes (data of Cherniak and Liang (2012, 2014) extrapolated at lower temperature). In contrast, diffusivity of Ti in amphibole appears to be at least one-order of magnitude slower than diffusivity of Zr in rutile (Cherniak et al. 2007; Fig. 15a). When Zr-in-rutile diffusivities from Sasaki et al. (1985) and Dohmen et al. (2019) are considered,

parameters for the diffusion of Ti through amphibole are still missing. Many recent studies focused on Ti diffusion in quartz and zircon due to the interest in applying Ti-in-quartz and Ti-in-zircon thermometers (e.g., Jollands et al. 2020; Bloch et al. 2022; Audétat et al. 2023). Some Ti diffusion data were also reported for pyroxene, feldspar and
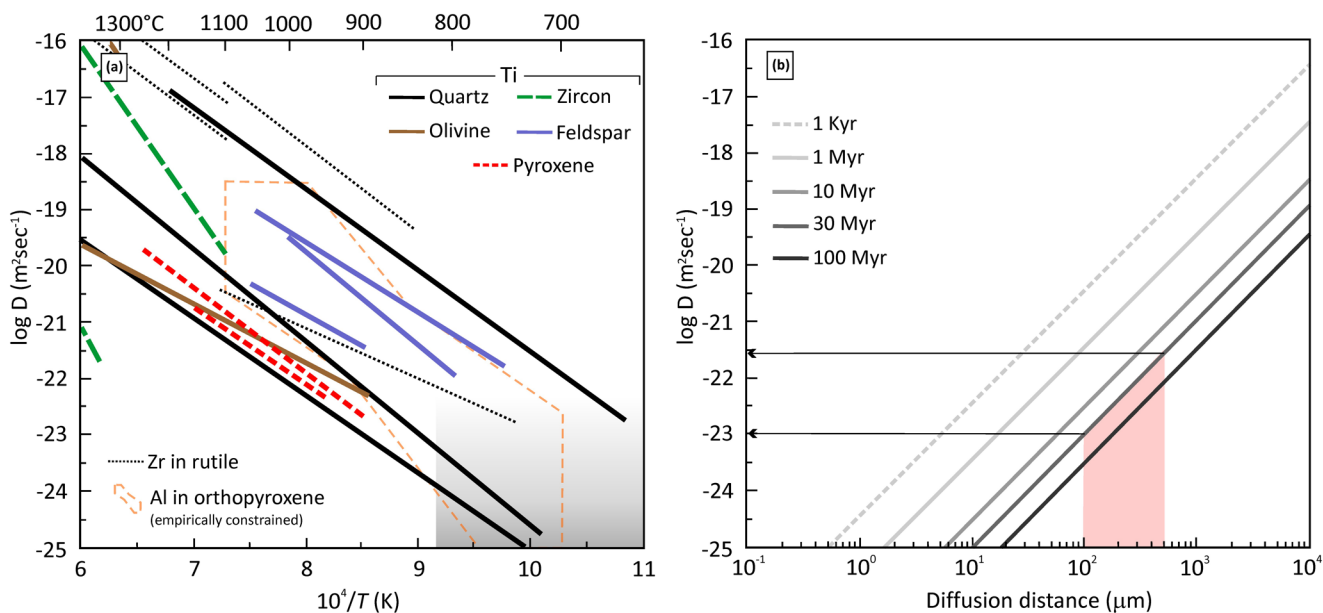
Fig. 15 (**a**) Arrhenius plot comparing the Ti-in-amphibole diffusivities inferred in this study (dashed grey area) against experimentally derived diffusivities of Ti in other minerals and Zr in rutile. Data from: Sasaki et al. (1985); Cherniak et al. (2007a, b); Cherniak and Watson (2020); Cherniak and Liang (2012, 2014); Jollands et al. (2016, 2020); Dohmen et al. (2019); Bloch et al. (2022); Audétat et al. (2021, 2023). Also, the Al diffusivities in orthopyroxene are reported (Smye et al. 2017). (**b**) Diffusivity (D) dependent diffusion distance (x), calculated for different durations. Red area refers to diffusion distances hypothesized for amphiboles from IVZ granulites

this difference is greater. Assuming Zr diffusivities in rutile of 10^{-23} m^{2}sec^{-1} at 750 °C (data from Cherniak et al. 2007), Zr-in-rutile temperatures should be reset in rutile crystals of ≈ 200 μm in size ($x = 100$ μm) which experienced ≈ 30 Myr of slow cooling between 800 and 700 °C (Fig. 15b). Regarding the IVZ, it is important to recall that the resetting of Zr-in-rutile thermometer was mostly explained by recrystallization, rather than diffusive re-equilibration (see above).

Despite the importance of Al content in orthopyroxene for thermometry of granulites (Harley and Green 1982; Clark et al. 2019), no experimental data are available for Al diffusion in orthopyroxene. Smye et al. (2017) derived some estimations on Al diffusivities based on REE-in-pyroxene speedometry. Although their calculations suffer from severe uncertainties, the potential overlap between diffusivities of Ti in amphibole and Al in orthopyroxene (Fig. 15a) is consistent with the fact that both Ti-in-amphibole and Al-in-orthopyroxene thermometers record UHT conditions (Fig. 14).

To our knowledge, this is the first study trying to infer some Arrhenian parameters for Ti diffusion in amphibole. However, the empirically constrained diffusivities reported above ($> 10^{-23}$ m^{2}sec^{-1} at 650–800 °C) have to be considered with caution. Their sound quantification demands experimental studies, which should also consider the possible effect of composition and anisotropy on diffusion. Modeling diffusive mass transport in amphibole will also require more complex solutions and simulations.

Conclusions

We applied the Ti-in-amphibole thermometer to ilmenite-bearing metabasites from the Ivrea–Verbano Zone (NW Italy) and the following conclusions can be drawn:

- The Ti content of amphibole is buffered by the presence of a Ti-phase (ilmenite, rutile, titanite), whereas the bulk rock TiO_2 content may have a second-order effect.
- Ti-in-amphibole thermometry returns progressively higher temperatures across the IVZ, compatible with the observed increase in metamorphic grade seen in the field.
- The Ti-in-amphibole thermometer, Zr-in-rutile thermometer, and phase equilibria modelling record peak conditions across the IVZ.
- The Zr-in-rutile thermometer is more prone to post-peak resetting when compared to Ti-in-amphibole thermometry in the IVZ granulites.
- The peak metamorphic Ti content of amphibole can be reset locally, in portions of rock significantly affected by retrograde fluid influx.

The robustness of the Ti-in-amphibole thermometer in recording UHT conditions is confirmed by other case studies and its performance is comparable with that of Al-in-orthopyroxene in pelitic granulites. However, Ti-in-amphibole thermometry underestimates temperature for

rocks equilibrated in the rutile stability field, whatever their H_2O content is. The empirically constrained Ti diffusivity in amphibole ($> 10^{-23}$ m^{2}sec^{-1} at 650–800 °C) indicates that Ti concentrations in amphibole will be less affected by later thermal disturbance than Zr concentrations in rutile, as indicated by natural occurrences. Future experimental studies are, however, necessary to develop a more robust calibration for the Ti-in-amphibole thermometer, in order to take into account the possible effect of a_{TiO2} and pressure and to extend its applicability.

Declarations

References

Acosta-Vigil A, London D, Morgan VIGB, Dewers TA (2006) Dissolution of quartz, albite, and orthoclase in H_2O-saturated haplogranitic melt at 800°C and 200 MPa: diffusive transport properties of granitic melts at crustal anatectic conditions. J Petrol 47/2:231–254

Ague JJ, Eckert JO (2012) Precipitation of rutile and ilmenite needles in garnet: implications for extreme metamorphic conditions in the Acadian Orogen, U.S.A. Am Mineral 97:840–855

Aidoo F, Zhang Q-Q, Zhang S-B, Nude PM (2022) Identification of UHT granulites in the pan-african Dahomeyide Suture Zone in SE Ghana: implications for evolution of collisional orogens. J Petrol 63/6:1–33

Audétat A, Miyajima N, Wiesner D, Audinot JN (2021) Confirmation of slow Ti diffusion in quartz by diffusion couple experiments and evidence from natural samples. Geology 49/8:963–967

Audétat A, Schmitt AK, Njul R, Saalfeld M, Borisova A, Lu Y (2023) New constraints on Ti diffusion in quartz and the priming of silicic volcanic eruptions. Nat Commun 14:4277

Backer DR (1992) Estimation of diffusion coefficients during interdifussion of geologic melts: application of transition state theory. Chem Geol 98:11–21

Barboza SA, Bergantz GW (2000) Metamorphism and anatexis in the mafic complex contact aureole, Ivrea Zone, northern Italy. J Petrol 41:1307–1327

Barboza SA, Bergantz GW, Brown M (1999) Regional Granulite facies metamorphism in the Ivrea zone: is the mafic Complex the smoking gun or a red herring? Geology 27:447–450

Bartoli O, Carvalho BB (2021) Anatectic granites in their source region: a comparison between experiments, thermodynamic modelling and nanogranitoids. Lithos 402–403:106046

Bea F, Montero P Behavior of accessory phases and redistribuition of Zr, REE, Y, Th (1999) and U during metamorphism and partial melting of metapelites in the lower crust: An example from the Kinzigite Formation of Ivrea-Verbano Zone, NW Italy. Geochimica et Cosmochimica Acta, 63:1133–1153

Bertolani M (1964a) Le Stronaliti. Rend Soc Mineral Ital 20:31–69

Bertolani M (1964b) Considerazioni Geopetrografiche sulla valle Strona. Atti Soc Tosc Sci Nat 71:1–20

Bertolani M (1964c) Le Metamorfiti dell'alta valle Strona (Provincia Di Novara). Period Mineral 33:302–332

Bertolani M (1968) La Petrografia della Valle Strona (Alpi Occidentali Italiane). Schweiz Mineral Petrogr Mitt 48:695–733

Bertolani M, Rivalenti G (1966) Gli gneiss anfibolici della Valle Strona. Period Mineral 35:869–896

Bloch EM, Jollands MC, Tollan P, Plane F, Bouvier A-S, Herving R, Berry AJ, Zaubitzer C, Escrig S, Müntener O et al (2022) Diffusion anisotropy of Ti in zircon and implications for Ti-in-zircon thermometry. Earth Planet Sc Lett 578:117317

Bohlen SR, Essene EJ (1979) A critical evaluation of two-pyroxene thermometry in Adirondack granulites. Lithos 12/4:335–345

Boriani AC, Villa IM (1997) Geochronology of regional metamorphism in the Ivrea-Verbano Zone and Serie dei Laghi, Italian Alps. Schweiz Mineral Petrogr Mitt 77(3):381–401

Boriani A, Burlini L, Sacchi R (1990) The Cossato-Mergozzo-Brissago line and the Pogallo line (Southern Alps, Northern Italy) and their relationships with the late-hercynian magmatic and metamorphic events. Tectonophysics 182:91–102

Brodie KH, Rutter EH (1987) Deep crustal extensional faulting in the Ivrea Zone of Northern Italy. Tectonophysics 140:193–212

Carvalho BB, Bartoli O, Ferri F, Cesare B, Ferrero S, Remusat L, Poli S (2019) Anatexis and fluid regime of the deep continental crust: new clues from melt and fluid inclusions in metapelitic migmatites from Ivrea Zone (NW Italy). J Metamorph Geol 37:951–975

Carvalho BB, Bartoli O, Cesare B, Tacchetto T, Gianola O, Ferri F, Szabó C (2020) Primary CO_2-bearing fluid inclusions in granulitic garnet usually do not survive. Earth Planet Sci Lett 536:116170

Carvalho BB, Bartoli O, Cesare B (2023a) C–O–H fluid-melt-rock interaction in graphitic granulites and problems of quantifying carbon budget in the lower continental crust. Chem Geol 631(1–2):121503

Carvalho BB, Bartoli O, Cesare B, Satish-Kumar M, Petrelli M, Kawakami T, Hokada T, Gilio M (2023b) Revealing the link between A-type granites and hottest melts from residual metasedimentary crust. Geology 51/9:845–849

Cherniak DJ, Liang Y (2012) Ti diffusion in natural pyroxene. Geochim Cosmochim Acta 98:31–47

Cherniak DJ, Liang Y (2014) Ti diffusion in olivine. Geochim Cosmochim Acta 147:43–57

Cherniak DJ, Watson EB (2020) Ti diffusion in feldspar. Am Mineral 105:1040–1050

Cherniak DJ, Watson EB, Wark DA (2007a) Ti diffusion in quartz. Chem Geol 236:65–74

Cherniak DJ, Manchester J, Watson EB (2007b) Zr and Hf diffusion in rutile. Earth Pl Sci Lett 261:267–279

Clark C, Fitzsimons ICW, Healy D, Harley SL (2011) How does the continental crust get really hot? Elements 7(4):235–240

Clark C, Taylor RJM, Johnson TE, Harley SM, Fitzsimons ICW, Oliver L (2019) Testing the fidelity of thermometers at ultrahigh temperatures. J Metamorph Geol 37:917–934

Clough PWL, Field D (1980) Chemical variation in metabasites from a proterozoic amphibolite-granulite transition zone, South Norway. Contrib Mineral Petrol 73:277–286

Connolly JAD (2009) The geodynamic equation of state: what and how. Geochem Geophys Geosyst 10:Q10014

Corvò S, Maino M, Piazolo S, Seno S, Langone A (2022) Role of inherited compositional and structural heterogeneity in shear zone development at mid-low levels of the continental crust (the Anzola shear zone; Ivrea-Verbano Zone, Southern Alps). Lithos 422–423:106745

De Angelis S, Larsen J, Coombs M (2013) Pre-eruptive magmatic conditions at augustine volcano, Alaska, 2006: evidence from amphibole geochemistry and textures. J Petrol 54/9:1939–1961

Dev JA, Tomson JK, Corcar N, Nandakumar V (2021) Combined U-Pb/Hf isotopic studies and phase equilibrium modelling of HT-UHT metapelites from Kambam ultrahigh-temperature belt, south India: constraints on tectonothermal history of the terrane. Lithos 406–407:106531

Dharmapriya P, Malaviarchchi SPK, Galli A, Kriegsman LM, Osanai Y, sajeev K, Su B-X, Tsunogae T et al (2021) Hybrid phase equilibria modelling with conventional and trace element thermobarometry to assess the P–T evolution of UHT granulites: an example from the Highland Complex, Sri Lanka. J Metamorph Geol 39/2:209–246

Dohmen R, Marschall HR, Ludwing T, Polednia J (2019) Diffusion of Zr, Hf, Nb and Ta in rutile: effects of temperature, oxygen fugacity, and doping level, and relation to rutile point defect chemistry. Phys Chem Mineral 46:311–332

Duan W-Y, Chen S, Schertl H-P, Li X-P (2023) High-pressure/ultra-high-temperature mafic and felsic granulites associated with magnetite deposits from the Jiaobei terrane, Jiao-Liao-Ji Belt, North China Craton. Lithos 152:105252

Ernst WG, Liu J (1998) Experimental phase-equilibrium study of Al- and Ti-contents of calcic amphibole in MORB—A semiquantitative thermobarometer. Am Mineral 83:952–969

Ewing TA, Hermann J, Rubatto D (2013) The robustness of the Zr-in-rutile and Ti-in-zircon thermometers during high-temperature metamorphism (Ivrea-Verbano Zone, Northern Italy). Contrib Mineral Petrol 165:757–779

Ewing TA, Rubatto D, Beltrando M, Hermann J (2015) Constraints on the thermal evolution of the Adriatic margin during jurassic continental break-up: U-Pb dating of rutile from the Ivrea-Verbano Zone, Italy. Contrib Min Petrol 169:44

Ferry JM, Watson EB (2007) New thermodynamic models and revised calibrations for the Ti-in-zircon and Zr-in-rutile thermometers. Contrib Mineral Petrol 154:429–437

Fonseca Texeira LM, Troch J, Bachmann O (2023) The dynamic nature of $aTiO_2$: Implications for Ti-based thermometers in magmatic systems. Geology

Forshaw JB, Waters DJ, Pattison DRM, Palin RM, Gopon P (2019) A comparison of observed and thermodynamically predicted phase equilibria and mineral compositions in mafic granulites. J Metamorph Geol 37/2:153–179

Franz L, Harlov DE (1998) High-grade K-feldspar veining in granulites from the Ivrea±Verbano Zone, northern Italy: fluid flow in the lower crust and implications for granulite facies genesis. J Geol 106:455–472

Frost BR, Chacko T (1989) The granulite uncertainty principle: limitations on thermobarometry in granulites. J Geol 97:435–450

García-Arias (2020) Consistency of the activity–composition models of Holland, Green, and Powell (2018) with experiments on natural and synthetic compositions: a comparative study. J Metamorph Geol 38/9:993–1010

Gianola O, Costa B, Ferri F, Gilio M, Petrelli M, Murri M, Alvaro M Rodriíguez-Vargas A, Poli S, Cesare B (2023) Melt inclusions in arclogitic xenoliths constrain the genesis of the lower continental arc crust beneath the Northern Volcanic Zone, Colombia. J Petrol 64:1–24

Govindaraju K (1994) Compilation of working values and sample description for 383 geostandard. Geostandards Newsl 18:1–158

Green ECR, White RW, Diener JFA, Powell R, Holland TJB, Palin RM (2016) Activity-composition relations for the calculation of partial melting equilibria in metabasic rocks. J Metamorph Geol 34/9:845–869

Handy MR, Franz L, Heller F, Janott B, Zurbriggen R (1999) Multistage accretion and exhumation of the continental crust (Ivrea crustal section, Italy and Switzerland). Tectonics 18/6:1154–1177

Harley SL (2021) UHT metamorphism. Encyclop Geol (2nd edition) 522–552

Harley SL, Green DH (1982) Garneteorthopyroxene barometry for granulites and peridotites Nature 300:697–701

Harlov DE, Förster H-J (2002) High-grade fluid metasomatism on both a local and regional scale: the Seward Peninsula, Alaska and the Val Strona Di Omegna, Ivrea-Verbano Zone, northern Italy: Part I. Petrography and silicate mineral chemistry. J Petrol 43:769–799

Harlov DE, Tropper P, Seifert W, Nijland T, Förster H-J (2006) Formation of Al-rich titanite ($CaTiSiO_4O$–$CaAlSiO_4OH$) reaction rims on ilmenite in metamorphic rocks as a function of f H_2O and fO_2. Lithos 88:72–84

Hart E, Storey C, Harley SL, Fowler M (2018) A window into the lower crust: trace element systematics and the occurrence of inclusions/intergrowths in granulite-facies rutile. Gondwana Res 59:76–86

Hawthorne FC, Oberti R, Harlow GE, Maresch WV, Martin RF, Schumacher JC, Welch MD (2012) Nomenclature of the amphibole supergroup. Am Mineral 97:2031–2048

He X-F, Hand M, Santosh M, Kelsey DE, Morrissey LJ, Tsunogae T (2021) Long-lived metamorphic P–T–t evolution of the Highland Complex, Sri Lanka: insights from mafic granulites. Precamb Res 316:227–243

Henk A, Franz L, Teufel S, Oncken O (1997) Magmatic underplating, extension, and crustal reequilibration: insights from a cross-section through the Ivrea Zone and Strona-Ceneri Zone, Northern Italy. J Geol 105:367–378

Holland T, Blundy J (1994) Non-ideal interactions in calcic amphiboles and their bearing on amphibole-plagioclase thermometry. Contrib Mineral Petrol 116:433–447

Holland TJB, Green ECR, Powell R (2018) Melting of peridotites through to granites: a simple thermodynamic model in the system KNCFMASHTOCr. J Petrol 59:881–900

Hollister LS, Grissom GC, Peters EK, Stowell HH, Sisson VB (1987) Confirmation of the empirical correlation of Al in hornblende with pressure of solidification of calc alkaline plutons. Am Mineral 72:231–239

Huang G, Guo J, Palin R (2021) Phase equilibria modeling of anatexis during ultra-high temperature metamorphism of the crust. Lithos 398–399:106326

Hunziker JC, Zingg A (1980) Lower palaeozoic amphibolite to granulite facies metamorphism in the Ivrea zone (Southern Alps, Northern Italy). Sch Mineral Petrogr Mitt 60:181–213

Jiao S, Brown M, Mitchell RN, Chowdhury P, Clark C, Chen L, Chen Y, Korhonen F, Huang G, Guo J (2023) Mechanisms to generate ultrahigh-temperature metamorphism. Nat Rev Earth Environ 4:298–318

Jollands MC, Hermann J, O'Neill HStCO, Spandler C, Padrón-Navarta JA (2016) Diffusion of Ti and some divalent cations in olivine as a function of temperature, oxygen fugacity, chemical potentials and crystal orientation. J Petrol 57/10:1983–2010

Jollands MC, Bloch E, Müntener O (2020) New Ti-in-quartz diffusivities reconcile natural Ti zoning with time scales and temperatures of upper crustal magma reservoirs. Geology 48:654–657

Karakas O, Wotzlaw J-F, Guillong M, Ulmer P, Brack P, Economos R, Bergantz GW, Sinigoi S, Bachmann O (2019) The pace of crustal-scale magma accretion and differentiation beneath silicic caldera volcanoes. Geology 47:719–723

Kelsey DE, Hand M (2015) On ultrahigh temperature crustal metamorphism: phase equilibria, trace element thermometry, bulk composition, heat sources, timescales and tectonic settings. Geosc Front 6(3):311–356

King PL, Hervig RL, Holloway JR, Vennemann TW, Righter K (1999) Oxy-substitution and dehydrogenation in mantle-derived amphibole megacrysts. Geoch Cosmoch Acta 63/21:3635–3651

Klötzli US, Sinigoi S, Quick JE, Demarchi G, Tassinari CC, Sato K, Günes Z (2014) Duration of igneous activity in the Sesia Magmatic System and implications for high-temperature metamorphism in the Ivrea-Verbano deep crust. Lithos 206–207:19–33

Kohn MJ (2020) A refined zirconium-in-rutile thermometer. Am Mineral 105:963–971

Korhonen FJ, Clark C, Brown M, Taylo RJM (2015) Taking the temperature of Earth's hottest crust. Earth Plan Sc Lett 408:341–354

Kunz BE, White RW (2019) Phase equilibrium modelling of the amphibolite to granulite facies transition in metabasic rocks (Ivrea Zone, NW Italy). J Metamorph Geol 37/7:935–950

Kunz BE, Johnson TE, White RW, Redler C (2014) Partial melting of metabasic rocks in Val Strona Di Omegna, Ivrea Zone, northern Italy. Lithos 190 191:1–12

Kunz BE, Regis D, Engi M (2018) Zircon ages in granulite facies rocks: decoupling from geochemistry above 850°C? Contrib Mineral Petrol 173:26

Lanari P, Duesterhoeft E (2019) Modeling metamorphic rocks using equilibrium thermodynamics and internally consistent databases: past achievements, problems and perspectives. J Petrol 60/1:19–56

Langone A, Padrón-Navarta JA, Ji W-Q, Zanetti A, Mazzucchelli M, Tiepolo M, Giovanardi T, Bonazzi M (2017) Ductile-brittle deformation effects on crystal-chemistry and U-Pb ages of magmatic and metasomatic zircons from a dyke of the Finero mafic complex (Ivrea-Verbano Zone, Italian Alps). Lithos 284–285:493–511

Leake BE (1965) The relationship between composition of calciferous amphibole and grade of metamorphism. In: Pitcher WS, Flinn GW (eds) Controls of Metamorphism. Wiley, New York, pp 299–318

Li L, Wang X-L, Yakymchuk C, Schorn S, Yu J-H, Wang D, Li J-Y, Du D-D, Huang Y (2022) A refined study of Paleoproterozoic high-pressure granulite-facies metamorphism in the Kongling complex of northern Yangtze block. Precambrian Res 378:106741

Liao Y, wei C, Rehman HU (2021) Titanium in calcium amphibole: behavior and thermometry. Am Mineral 106:180–191

Liu Z, Carvalho BB, Li W, Tong L, Bartoli O, Chen L, Yan Q, Wu H (2023) Into the high to ultrahigh temperature melting of earth's crust: investigation of melt and fluid inclusions within Mg-rich metapelitic granulites from the Mather Peninsula, East Antarctica. J Petrol 64(7):1–27

Luvizotto GL, Zack T (2009) Nb and zr behavior in rutile during high-grade metamorphism and retrogression: an example from the Ivrea–Verbano Zone. Chem Geol 261(3/4):303–317

Mazzuchelli M, Siena F (1986) Geotectonic significance of the metabasites of the Kinzigitic Series, Ivrea-Verbano Zone (Western Italian Alps). TMPM Tschermaks Min Petr Mitt 35:99–116

Mazzuchelli M, Rivalenti G, Vannucci R, Bottazzi P, Ottolini L, Hofmann AW, Parenti M (1992) Primary positive Eu anomaly in clinopyroxenes of low-crust gabbroic rocks. Geoch Cosmoch Acta 56/6:2363–2370

Mitchell RJ, Harley SL (2017) Zr-in-rutile resetting in aluminosilicate bearing ultra-high temperature granulites: refining the record of cooling and hydration in the Napier Complex, Antarctica. Lithos 272–273:128–146

Osanai Y, Sajeev K, Nakano N, Kitano I, Kehelpannala WKV, Kato R, Adachi T, Malaviarachchi PK (2016) UHT granulites of the Highland Complex, Sri Lanka I: geological and petrological background. J Mineral Petrol Sci 111:145–156

Otten MT (1984) The origin of brown hornblende in the Artfj illet gabbro and dolerites. Contr Min Petrol 86:189–199

Palin RM, White RW, Green ECR (2016) Partial melting of metabasic rocks and the generation of tonalitic–trondhjemitic–granodioritic (TTG) crust in the Archean: constraints from phase equilibrium modelling. Precambrian Res 287:73–90

Pape J, Mezger K, Robyr M (2016) A systematic evaluation of the Zr–in–rutile thermometer in ultra–high temperature (UHT) rocks. Contrib Mineral Petrol 171:44

Pattison DRM, Chacko T, Farquhar J, Mcfarlane CM (2003) Temperatures of granulite-facies metamorphism: constraints from experimental phase equilibria and thermobarometry corrected for retrograde exchange. J Petrol 44:867–900

Pattison DRM, Chacko T, Farquhar J, McFarlane CRM, Widney J (2019) Program RCLC: garnet–orthopyroxene thermobarometry corrected for late Fe–Mg exchange. J Petrol 60:1107–1108

Peressini G, Quick JE, Sinigoi S, Hofmann AW, Fanning M (2007) Duration of a large mafic intrusion and heat transfer in the lower crust: a SHRIMP U–Pb zircon study in the Ivrea-Verbano Zone (Western Alps, Italy). J Petrol 48:1185–1218

Plumper O, Botan A, Los A, Liu Y, Malthe-Sorenssen A, Jamtveit B (2017) Fluid-driven metamorphism of the continental crust governed by nanoscale fluid flow. Nat Geoscience 10:685–690

Powell R, Holland TJB (2008) On thermobarometry. J Metamorph Geol 26(2):155–179

Prakash D, Prakash S, Sachan HK (2010) Petrological evolution of the high pressure and ultrahigh-temperature mafic granulites from Karur, southern India: evidence for decompressive and cooling retrograde trajectories. Min Petrol 100:35–53

Qi Y, Kohn MJ, Huang G, Zhen Y, Jiao S, Guo J (2022) Thermal regime of the lower crust in the eastern Khondalite Belt, North China Craton, constrained by Zr-in-rutile thermometry mapping. Precambrian Res 377:106720

Quick JE, Sinigoi S, Mayer A (1995) Emplacement of mantle peridotite in the lower continental crust, Ivrea-Verbano Zone, northern Italy. Geology 23:739–742

Quick JE, Sinigoi S, Snoke AW, Kalakay TJ, Mayer A, Peressini G (2003) Geologic map of the southern Ivrea-Verbano Zone northwestern Italy. U.S. Geological Survey, Geologic Investigations Series Map I-2776, scale 1:25,000

Raase P (1974) A1 and Ti contents of hornblende, indicators of pressure and temperature of regional metamorphism. Contr Mineral Petrol 45:231–236

Raase P, Raith M, Ackermand D, Lal R (1986) Progressive metamorphism of mafic rocks from greenschist to granulite facies in the Dharwar Craton of South India. J Geol 94:261–282

Raith M, Raase P (1986) High grade metamorphism in the granulite belt of Finnish Lapland. Geolog Soc Lond Spec Public 24:283–295

Rapp RP, Watson EB (1995) Dehydration melting of metabasalt at 8–32 kbar: implications for continental growth and crust-mantle recycling. J Petrol 36:891–931

Ray S, Tiwari AK, Sarkar T (2021) Ultrahigh-temperature mafic granulites from the Madurai Block, southern India: constraints from conventional thermobarometry, pseudosection analysis, and rare earth element-based thermometry. Geol J 56:3720–3744

Redler C, Johnson TE, White RW, Kunz BE (2012) Phase equilibrium constraints on a deep crustal metamorphic field gradient: metapelitic rocks from the Ivrea Zone (NW Italy): Ivrea Zone metamorphic field gradient. J Metamorph Geol 30:235–254

Redler C, White RW, Johnson TE (2013) Migmatites in the Ivrea Zone (NW Italy): constraints on partial melting and melt loss in metasedimentary rocks from Val Strona Di Omegna. Lithos 175–176:40–53

Reinsch D (1973) Die Metabasite Des Valle Strona (Ivrea Zone). Neues Jahrbuch Mineralogische Abhandlungen 118:190–210

Ridolfi F, Zanetti A, Renzulli A, Perugini D, Holtz F, Oberti R (2018) AMFORM, a new mass-based model for the calculation of the unit formula of amphiboles from electron microprobe analyses. Am Mineral 103(7):1112–1125

Rivalenti G, Garuti G, Rossi A (1975) The origin of the Ivrea-Verbano basic formation (western Italian Alps); whole rock geochemistry. Boll Soc Geol It 94:1149–1186

Rushmer T (1991) Partial melting of two amphibolites: contrasting experimental results under fluid-absent conditions. Contrib Min Petrol 107:41–59

Rutter E, Brodie K, James T, Burlini L (2007) Large-scale folding in the upper part of the Ivrea-Verbano Zone, NW Italy. J Struct Geol 29:1–17

Sajeev K, Osanai Y (2004) Ultrahigh-temperature metamorphism (1150°C, 12 kbar) and multistage evolution of Mg-,Al-rich granulites from the Central Highland Complex, Sri Lanka. J Petrol 45(9):1821–1844

Sajeev K, Osanai Y, Kon Y, Itaya T (2009) Stability of pargasite during ultrahigh-temperature metamorphism: a consequence of titanium and REE partitioning? Am Mineral 94:535–545

Santos CA, Moraes R, Szabo GAJ (2019) A comparison between phase diagram modeling of metamafic rocks and experimental and independent thermobarometric data. Lithos 340–341:108–123

Sasaki J, Peterson NL, Hoshino K (1985) Tracer impurity diffusion in single-crystal rutile (TiO_{2-x}). J Phys Chem Solids 46:1267–1283

Sawyer EW (1991) Disequilibrium melting and the rate of melt–residuum separation during migmatization of mafic rocks from the Grenville Front, Quebec. J Petrol 32:701–738

Sawyer EW (2008) Atlas of migmatites (Vols. The Canadian mineralogist, Special publications 9) (E. W. Sawyer Ed). NRC Research, Ottawa, Canada

Schmid SM (1993) Ivrea Zone and adjacent Southern Alpine Basement. In: Raumer JF, Neubauer F (eds) Pre-mesozoic geology in the Alps. Springer, Berlin, Heidelberg, pp 567–585

Schmid R, Wood BJ (1976) Phase relationships in granulitic metapelites from the Ivrea-Verbano zone (Northern Italy). Contrib Mineral Petrol 54:255–279

Schmid SM, Zingg A, Handy M (1987) The kinematics of movements along the Insubric line and the emplacement of the Ivrea Zone. Tectonophysics 135:47–66

Schmidt MW (1992) Amphibole composition in tonalite as a function of pressure: an experimental calibration of the Al-in-hornblende barometer. Contrib Mineral Petrol 110:304–310

Schnetger B (1994) Partial melting during the evolution of the amphibolite-to granulite-facies gneisses of the Ivrea Zone, northern Italy. Chem Geol 113:71–101

Schorn S, Diener JFA (2019) Seemingly disparate temperatures recorded in coexisting granulite facies lithologies. J Metamorph Geol 37:1049–1078

Shimizu H, Tsunogae T (2021) Zr-in-rutile geothermometry of sapphirine + quartz–bearing ultrahigh-temperature granulites from Rajapalaiyam in the Madurai Block, southern India. Earth Evolut Sci 15:11–17

Siegesmund S, Layer P, Dunkl I, Vollbrecht A, Steenken A, Wemmer K, Ahrendt H (2008) Exhumation and deformation history of the lower crustal section of the Valstrona Di Omegna in the Ivrea Zone, southern Alps. Geol Soc Lond Spec Publ 298:45–68

Sills JD (1984) Granulite facies metamorphism in the Ivrea Zone, NW Italy. Sch Mineral Petrogr Mitt 64:69–91

Sills JD, Tarney J (1984) Petrogenesis and tectonic significance of amphibolites interlayered with metasedimentary gneisses in the Ivrea Zone, Southern Alps, northwest Italy. Tectonophysics 3–4:187–206

Simonetti M, Langone A, Bonazzi M, Corvò S, Maino M (2023) Tectono-metamorphic evolution of a post-variscan mid-crustal shear zone in relation to the Tethyan rifting (Ivrea-Verbano Zone, Southern Alps). J Struct Geol 173:104896

Sinigoi S, Antonini P, Demarchi G, Longinelli A, Mazzucchelli M, Negrini L, Rivalenti G (1991) Intractions of mantle and crustal magmas in the southern part of the Ivrea Zone (Italy). Contrib Min Petrol 108:385–395

Sinigoi S, Quick JE, Clemens-Knott D, Mayer A, Demarchi G, Mazzucchelli M, Nehrini L, Rivalenti G (1994) Chemical evolution of a large mafic intrusion in the lower crust, Ivrea-Verbano Zone, northern Italy. J Geoph Res 99:21:575–21590

Sinigoi S, Quick JE, Mayer A, Budahn J (1996) Influence of stretching and density contrasts on the chemical evolution of continental magmas: an example from the Ivrea-Verbano Zone. Contrib Min Petrol 123:238–250

Smye AJ, Stockli DF (2014) Rutile U-Pb age depth profiling: a continuous record of lithospheric thermal evolution. Earth Planet Sci Lett 408:171–182

Smye A, Seman S, Hudak M, Crispin K (2017) Rates of mantle cooling and exhumation during rifting constrained by REE-in-pyroxene speedometry. Geochem Geophys Geosyst 18/7:2510–2525

Smye AJ, Lavier LL, Zack T, Stockli DF (2019) Episodic heating of continental lower crust during extension: a thermal modeling investigation of the Ivrea-Verbano Zone. Earth Planet Sci Lett 521:158–168

Spear FS (1981) An experimental study of hornblende stability and compositional variability in amphibolite. Am J Sc 281:697–734

Spear FS (1991) On the interpretation of peak metamorphic temperatures in light of granet diffusion during cooling. J Metamorph Geol 9/4:379–388

Tamashiro I, Santosh M, Sajeev K, Morimoto T, Tsunogae (2004) Zr-in-rutile geothermometry of sapphirine + quartz–bearing ultrahigh-temperature granulites from Rajapalaiyam in the Madurai Block, southern India. J Mineral Petrol Sci 99:279–297

Thomas W, Ernst WG (1990) The Aluminum Content of Hornblende in Calcalkaline Granitic Rocks; a Mineralogic Barometer Calibrated Experimentally to 12 kbars. In: Spencer, R.J. and Chou, I.-M., Eds., Fluid-Mineral Interactions: A Tribute to H.P. Eugster, Geochemical Society Special Publications, Geochemical Society, Washington DC, Vol. 2, 59–63

Tomkins HS, Powell R, Ellis DJ (2007) The pressure dependence of the zirconium-in-rutile thermometer. J Metamorph Geol 25:703–713

Vavra G, Schmid R, Gebauer D (1999) Internal morphology, habit and u-th-pb microanalysis of amphibolite-to-granulite facies zircons: geochronology of the Ivrea Zone (Southern Alps). Contrib Min Petrol 134:380–404

Voshage H, Hofmann AW, Mazzucchelli M, Rivalenti G, Sinigoi S, Raczek I, Demarchi G (1990) Isotopic evidence from the Ivrea Zone for a hybrid lower crust formed by magmatic underplating. Nature 347(6295):731–736

Waters DJ (1988) Partial melting and the formation of granulite facies assemblages in Namaqualand, South Africa. J Metamorph Geol 6:387–404

Watson EB (1982) Basalt contamination by continental crust: some experiments and models. Mineral Petrol 80:73–87

Watson EB, Jurewicz SR (1984) Behavior of alkalies during diffusive interaction of granitic xenoliths with basaltic magma. J Geolog 92:121–131

Watson EB, Wark DA, Thomas JB (2006) Crystallization thermometers for zircon and rutile. Contrib Mineral Petrol 151(4):413–433

Wheller CJ, Powell R (2014) A new thermodynamic model for sapphirine: calculated phase equilibria in K_2O–FeO–MgO–Al_2O_3–SiO_2–H_2O–TiO_2–Fe_2O_3. J Metamorph Geol 32:287–299

Williams MA, Kelsey DE, Rubatto D (2022) Thorium zoning in monazite: a case study from the Ivrea–Verbano Zone, NW Italy. J Metamorph Geol 40/6:1015–1042

Wolf MB, Wyllie PJ (1993) Dehydration-melting of amphibolite at 10 kbar: the effects of temperature and time. Contrib Mineral Petrol 115:369–383

Wolff R, Dunkl I, Kiesselbach G, Wemmer K, Siegesmund S (2012) Thermochronological constraints on the multiphase exhumation history of the Ivrea-Verbano Zone of the Southern Alps. Tectonophysics 579:104–117

Wyatt DC, James AJ, Garber JM, Hacker BR (2022) Assembly and tectonic evolution of continental lower crust: monazite petrochronology of the Ivrea-Verbano zone (Val Strona Di Omegna). Tectonics 41/3: e2021TC006841

Yakymchuk C, Brown M (2014) Behaviour of zircon and monazite during crustal melting. J Geol Soc 171:465–479

Zack T, Moraes R, Kronz A (2004) Temperature dependence of zr in rutile: empirical calibration of a rutile thermometer. Contrib Mineral Petrol 148:471–488

Zingg A (1980) Regional Metamorphism in the Ivrea Zone (Southern Alps, N-Italy): field and microscopic investigations. Sch Mineral Petrogr Mitt 60:153–179

Zingg A (1983) The Ivrea and Strona-Ceneri zones (Southern Alps, Ticino and N-Italy) – a review. Sch Mineral Petrogr Mitt 63:361–392

Zingg A, Handy MR, Hunziker JC, Schmid SM (1990) Tectonometamorphic history of the Ivrea Zone and its relationship to the crustal evolution of the Southern Alps. Tectonophysics 182:169–192